Monte-Carlo simulation of the strongly interacting Electroweak Chiral Lagrangian

R.L.Delgado, A.Dobado, D.Espriu, C.Garcia-Garcia, M.J.Herrero, X.Marcano and J.J.Sanz-Cillero

Universidad Complutense de Madrid

Presented at:

Multi-Boson Interactions 2017, KIT, Karlsruhe (Germany)

Based on arXiv:1707.04580 [hep-ph]

Standard lore

- The gauge bosons $W^{\pm}$ and Z are massive.
- This is problematic: the massive terms are not gauge invariant. Gauge boson scattering amplitudes diverge with s at LO.
- Standard Model solution: Higgs-mechanism, which predicts the SM Higgs boson. Global symmetry breaking pattern: $SU(2)_L \times SU(2)_R \to SU(2)_C$.
- In 2012, ATLAS and CMS find a 125-126 GeV scalar resonance h, compatible with the Higgs of the SM.

Standard lore

- The gauge bosons $W^{\pm}$ and Z are massive.
- This is problematic: the massive terms are not gauge invariant. Gauge boson scattering amplitudes diverge with s at LO.
- Standard Model solution: Higgs-mechanism, which predicts the SM Higgs boson. Global symmetry breaking pattern: $SU(2)_L \times SU(2)_R \to SU(2)_C$.
- In 2012, ATLAS and CMS find a 125-126 GeV scalar resonance h, compatible with the Higgs of the SM.

Standard lore

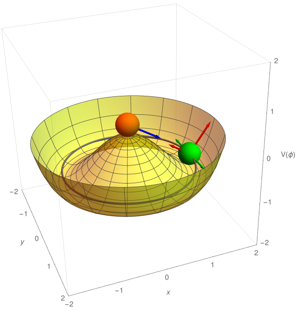

- The gauge bosons $W^{\pm}$ and Z are massive.
- This is problematic: the massive terms are not gauge invariant. Gauge boson scattering amplitudes diverge with s at LO.
- Standard Model solution:
  Higgs-mechanism, which predicts the SM Higgs boson. Global symmetry breaking pattern: $SU(2)_L \times SU(2)_R \to SU(2)_C$.
- In 2012, ATLAS and CMS find a 125-126 GeV scalar resonance h, compatible with the Higgs of the SM.

Standard lore

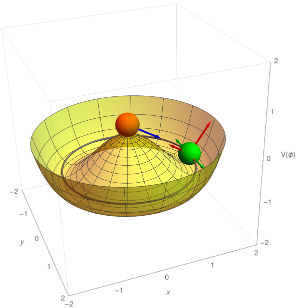

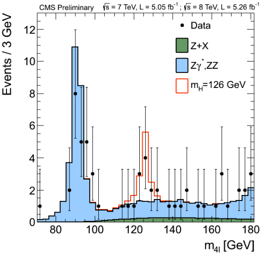

Phys. Lett. **B716**, 30-61.

- The gauge bosons $W^{\pm}$ and Z are massive.
- This is problematic: the massive terms are not gauge invariant. Gauge boson scattering amplitudes diverge with s at LO.
- Standard Model solution:
  Higgs-mechanism, which predicts the SM Higgs boson. Global symmetry breaking pattern: $SU(2)_L \times SU(2)_R \to SU(2)_C$.
- In 2012, ATLAS and CMS find a 125-126 GeV scalar resonance h, compatible with the Higgs of the SM.

Empirical situation

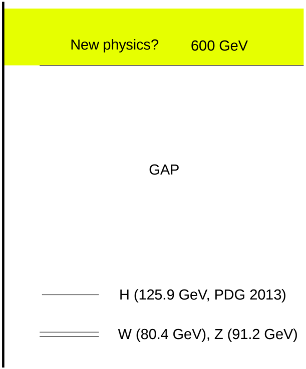

- AND: No new physics!!
  If there is any...
- The SM until the Planck mass?
- Some issues: mass of neutrinos, gravity explanation (*naturalness problem*), astrophysical observation (dark matter, dark energy),...
- Four scalar light modes, a large gap.
- Natural: further spontaneous symmetry breaking at $f > v = 246\,\mathrm{GeV}$?

Empirical situation

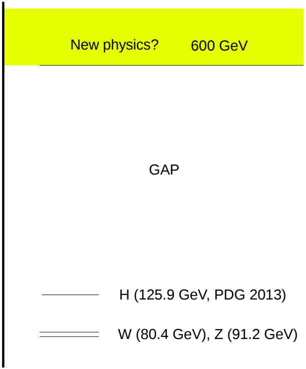

- AND: No new physics!!
  If there is any...
- The SM until the Planck mass?
- Some issues: mass of neutrinos, gravity explanation (*naturalness problem*), astrophysical observation (dark matter, dark energy),...
- Four scalar light modes, a large gap.
- Natural: further spontaneous symmetry breaking at $f > v = 246\,\mathrm{GeV}$?

Empirical situation

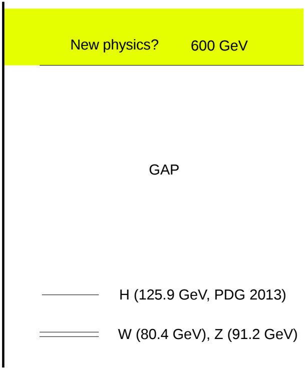

- AND: No new physics!!
  If there is any...
- The SM until the Planck mass?
- Some issues: mass of neutrinos, gravity explanation (*naturalness problem*), astrophysical observation (dark matter, dark energy),...
- Four scalar light modes, a large gap.
- Natural: further spontaneous symmetry breaking at $f > v = 246\,\text{GeV}$?

Empirical situation

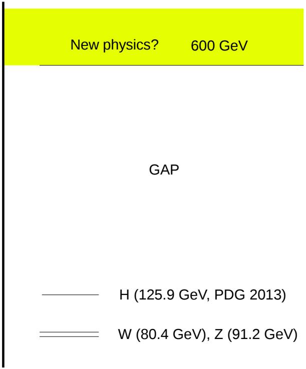

- AND: No new physics!!
  If there is any...
- The SM until the Planck mass?
- Some issues: mass of neutrinos, gravity explanation (*naturalness problem*), astrophysical observation (dark matter, dark energy),...
- Four scalar light modes, a large gap.
- Natural: further spontaneous symmetry breaking at $f > v = 246\,\mathrm{GeV}$?

Empirical situation

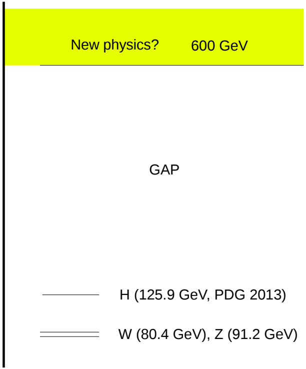

- AND: No new physics!!
  If there is any...
- The SM until the Planck mass?
- Some issues: mass of neutrinos, gravity explanation (*naturalness problem*), astrophysical observation (dark matter, dark energy),...
- Four scalar light modes, a large gap.
- Natural: further spontaneous symmetry breaking at $f > v = 246\,\mathrm{GeV}$?

Theoretical Study of the TeV scale

- From Top to Bottom: construct a full theory (renormalizable and UV complete), and describe the TeV scale in terms of the parameters of the BSM Lagrangian. For instance: MSSM has $\sim$ 100 free parameters.
  - Advantage: a full model. Renormalizability.
  - Problems: no hints about the UV completion chosen by nature.
  - Examples: MSSM ($\sim$ 100 free parameters), non-MSSM SUSY, Technicolor, KK,...
- From Bottom to Top: construct an Effective Field Theory (EFT), based on the symmetries and available degrees of freedom at low energy.
  - Advantage: we do not rely on a specific UV completion.
  - Disadvantage: valid only below certain energy scale. Non-renormalizable in the usual QFT sense, but renormalizable in the ChPT sense.
  - The usual EFT approach breaks when the low energy EFT reaches the unitarity bound, becoming non-perturbative.
  - For phenomenology, EFTs with the BSM physics (resonances) as explicit degrees of freedom are used.

Theoretical Study of the TeV scale

- From Top to Bottom: construct a full theory (renormalizable and UV complete), and describe the TeV scale in terms of the parameters of the BSM Lagrangian. For instance: MSSM has $\sim$ 100 free parameters.
  - Advantage: a full model. Renormalizability.
  - Problems: no hints about the UV completion chosen by nature.
  - Examples: MSSM ($\sim$ 100 free parameters), non-MSSM SUSY, Technicolor, KK,...
- From Bottom to Top: construct an Effective Field Theory (EFT), based on the symmetries and available degrees of freedom at low energy.
  - Advantage: we do not rely on a specific UV completion.
  - Disadvantage: valid only below certain energy scale. Non-renormalizable in the usual QFT sense, but renormalizable in the ChPT sense.
  - The usual EFT approach breaks when the low energy EFT reaches the unitarity bound, becoming non-perturbative.
  - For phenomenology, EFTs with the BSM physics (resonances) as explicit degrees of freedom are used.

Theoretical Study of the TeV scale

- From Top to Bottom: construct a full theory (renormalizable and UV complete), and describe the TeV scale in terms of the parameters of the BSM Lagrangian. For instance: MSSM has ~ 100 free parameters.
  - Advantage: a full model. Renormalizability.
  - Problems: no hints about the UV completion chosen by nature.
  - Examples: MSSM (~ 100 free parameters), non-MSSM SUSY, Technicolor, KK,...
- From Bottom to Top: construct an Effective Field Theory (EFT), based on the symmetries and available degrees of freedom at low energy.
  - Advantage: we do not rely on a specific UV completion.
  - Disadvantage: valid only below certain energy scale. Non-renormalizable in the usual QFT sense, but renormalizable in the ChPT sense.
  - The usual EFT approach breaks when the low energy EFT reaches the unitarity bound, becoming non-perturbative.
  - For phenomenology, EFTs with the BSM physics (resonances) as explicit degrees of freedom are used.

Theoretical Study of the TeV scale

- From Top to Bottom: construct a full theory (renormalizable and UV complete), and describe the TeV scale in terms of the parameters of the BSM Lagrangian. For instance: MSSM has ~ 100 free parameters.
  - Advantage: a full model. Renormalizability.
  - Problems: no hints about the UV completion chosen by nature.
  - Examples: MSSM (~ 100 free parameters), non-MSSM SUSY, Technicolor, KK,...
- From Bottom to Top: construct an Effective Field Theory (EFT), based on the symmetries and available degrees of freedom at low energy.
  - Advantage: we do not rely on a specific UV completion.
  - Disadvantage: valid only below certain energy scale. Non-renormalizable in the usual QFT sense, but renormalizable in the ChPT sense.
  - The usual EFT approach breaks when the low energy EFT reaches the unitarity bound, becoming non-perturbative.
  - For phenomenology, EFTs with the BSM physics (resonances) as explicit degrees of freedom are used.

Theoretical Study of the TeV scale

- From Top to Bottom: construct a full theory (renormalizable and UV complete), and describe the TeV scale in terms of the parameters of the BSM Lagrangian. For instance: MSSM has ~ 100 free parameters.
  - Advantage: a full model. Renormalizability.
  - Problems: no hints about the UV completion chosen by nature.
  - Examples: MSSM (~ 100 free parameters), non-MSSM SUSY, Technicolor, KK,...
- From Bottom to Top: construct an Effective Field Theory (EFT), based on the symmetries and available degrees of freedom at low energy.
  - Advantage: we do not rely on a specific UV completion.
  - Disadvantage: valid only below certain energy scale. Non-renormalizable in the usual QFT sense, but renormalizable in the ChPT sense.
  - The usual EFT approach breaks when the low energy EFT reaches the unitarity bound, becoming non-perturbative.
  - For phenomenology, EFTs with the BSM physics (resonances) as explicit degrees of freedom are used.

Theoretical Study of the TeV scale

- From Top to Bottom: construct a full theory (renormalizable and UV complete), and describe the TeV scale in terms of the parameters of the BSM Lagrangian. For instance: MSSM has ~ 100 free parameters.
  - Advantage: a full model. Renormalizability.
  - Problems: no hints about the UV completion chosen by nature.
  - Examples: MSSM (~ 100 free parameters), non-MSSM SUSY, Technicolor, KK,...
- From Bottom to Top: construct an Effective Field Theory (EFT), based on the symmetries and available degrees of freedom at low energy.
  - Advantage: we do not rely on a specific UV completion.
  - Disadvantage: valid only below certain energy scale. Non-renormalizable in the usual QFT sense, but renormalizable in the ChPT sense.
  - The usual EFT approach breaks when the low energy EFT reaches the unitarity bound, becoming non-perturbative.
  - For phenomenology, EFTs with the BSM physics (resonances) as explicit degrees of freedom are used.

Theoretical Study of the TeV scale

- From Top to Bottom: construct a full theory (renormalizable and UV complete), and describe the TeV scale in terms of the parameters of the BSM Lagrangian. For instance: MSSM has $\sim$ 100 free parameters.
  - Advantage: a full model. Renormalizability.
  - Problems: no hints about the UV completion chosen by nature.
  - Examples: MSSM ($\sim$ 100 free parameters), non-MSSM SUSY, Technicolor, KK,...
- From Bottom to Top: construct an Effective Field Theory (EFT), based on the symmetries and available degrees of freedom at low energy.
  - Advantage: we do not rely on a specific UV completion.
  - Disadvantage: valid only below certain energy scale. Non-renormalizable in the usual QFT sense, but renormalizable in the ChPT sense.
  - The usual EFT approach breaks when the low energy EFT reaches the unitarity bound, becoming non-perturbative.
  - For phenomenology, EFTs with the BSM physics (resonances) as explicit degrees of freedom are used.

Theoretical Study of the TeV scale

- From Top to Bottom: construct a full theory (renormalizable and UV complete), and describe the TeV scale in terms of the parameters of the BSM Lagrangian. For instance: MSSM has ~ 100 free parameters.
  - Advantage: a full model. Renormalizability.
  - Problems: no hints about the UV completion chosen by nature.
  - Examples: MSSM (~ 100 free parameters), non-MSSM SUSY, Technicolor, KK,...
- From Bottom to Top: construct an Effective Field Theory (EFT), based on the symmetries and available degrees of freedom at low energy.
  - Advantage: we do not rely on a specific UV completion.
  - Disadvantage: valid only below certain energy scale. Non-renormalizable in the usual QFT sense, but renormalizable in the ChPT sense.
  - The usual EFT approach breaks when the low energy EFT reaches the unitarity bound, becoming non-perturbative.
  - For phenomenology, EFTs with the BSM physics (resonances) as explicit degrees of freedom are used.

Theoretical Study of the TeV scale

- From Top to Bottom: construct a full theory (renormalizable and UV complete), and describe the TeV scale in terms of the parameters of the BSM Lagrangian. For instance: MSSM has ~ 100 free parameters.
  - Advantage: a full model. Renormalizability.
  - Problems: no hints about the UV completion chosen by nature.
  - Examples: MSSM (~ 100 free parameters), non-MSSM SUSY, Technicolor, KK,...
- From Bottom to Top: construct an Effective Field Theory (EFT), based on the symmetries and available degrees of freedom at low energy.
  - Advantage: we do not rely on a specific UV completion.
  - Disadvantage: valid only below certain energy scale. Non-renormalizable in the usual QFT sense, but renormalizable in the ChPT sense.
  - The usual EFT approach breaks when the low energy EFT reaches the unitarity bound, becoming non-perturbative.
  - For phenomenology, EFTs with the BSM physics (resonances) as explicit degrees of freedom are used.

EFTs + Unitarization Procedures

- We are interested in the collider phenomenology of Vector Bosons Scattering ($WZ \to WZ$), since it is very sensitive to new physics in the EW sector in the LHC.
- Bottom to Top approach: we construct an EFT for the EW sector. $SU(2)_L \times SU(2)_R$, EChL copy of ChPT in QCD.
- Degrees of freedom: Gauge Bosons $W^{\pm}$, Z + Higgs-like particle (h).
- 4 considered parameters: a, $b = a^2$, a_4, a_5.
- The NLO-computed EFT grows with the CM energy like $A \sim s^2$. Hence, it will eventually reach the unitarity bound, becoming non-perturbative. Options:
  - Limit the validity range of the EFT to the perturbative region. Consider it as a useful parameterization of slight deviations from the SM in the range under the TeV scale.
  - Take advantage of the analytical properties of the S-Matrix (encoded inside dispersion relations and unitarization procedures) to study the non-perturbative region (TeV scale) of the theory.

EFTs + Unitarization Procedures

- We are interested in the collider phenomenology of Vector Bosons Scattering ($WZ \to WZ$), since it is very sensitive to new physics in the EW sector in the LHC.
- Bottom to Top approach: we construct an EFT for the EW sector. $SU(2)_L \times SU(2)_R$, EChL copy of ChPT in QCD.
- Degrees of freedom: Gauge Bosons $W^{\pm}$, Z + Higgs-like particle (h).
- 4 considered parameters: a, $b = a^2$, a_4, a_5.
- The NLO-computed EFT grows with the CM energy like $A \sim s^2$. Hence, it will eventually reach the unitarity bound, becoming non-perturbative. Options:
  - Limit the validity range of the EFT to the perturbative region. Consider it as a useful parameterization of slight deviations from the SM in the range under the TeV scale.
  - Take advantage of the analytical properties of the S-Matrix (encoded inside dispersion relations and unitarization procedures) to study the non-perturbative region (TeV scale) of the theory.

EFTs + Unitarization Procedures

- We are interested in the collider phenomenology of Vector Bosons Scattering ($WZ \to WZ$), since it is very sensitive to new physics in the EW sector in the LHC.
- Bottom to Top approach: we construct an EFT for the EW sector. $SU(2)_L \times SU(2)_R$, EChL copy of ChPT in QCD.
- Degrees of freedom: Gauge Bosons $W^{\pm}$, Z + Higgs-like particle (h).
- 4 considered parameters: a, $b = a^2$, a_4, a_5.
- The NLO-computed EFT grows with the CM energy like $A \sim s^2$. Hence, it will eventually reach the unitarity bound, becoming non-perturbative. Options:
  - Limit the validity range of the EFT to the perturbative region. Consider it as a useful parameterization of slight deviations from the SM in the range under the TeV scale.
  - Take advantage of the analytical properties of the S-Matrix (encoded inside dispersion relations and unitarization procedures) to study the non-perturbative region (TeV scale) of the theory.

EFTs + Unitarization Procedures

Effective Lagrangian: considered parameters

$$\mathcal{L}_2 = \frac{v^2}{4}\left[1 + 2a\frac{h}{v} + b\left(\frac{h}{v}\right)^2 + \dots\right]\mathrm{Tr}(D_\mu U^\dagger D_\mu U) + \frac{1}{2}\partial_\mu h \partial^\mu h + \dots$$

$$\mathcal{L}_4 = a_4[\mathrm{Tr}(V_\mu V_\nu)][\mathrm{Tr}(V^\mu V^\nu)] + a_5[\mathrm{Tr}(V_\mu V^\mu)][\mathrm{Tr}(V_\nu V^\nu)] + \dots$$

$$V_\mu = (D_\mu U)U^\dagger, \qquad U = \exp\left(\frac{i\omega^a \tau^a}{v}\right)$$

Bosons

hysics in

/ sector.

article (h).

- 4 considered parameters: a, $b = a^2$, a_4, a_5.
- The NLO-computed EFT grows with the CM energy like $A \sim s^2$. Hence, it will eventually reach the unitarity bound, becoming non-perturbative. Options:
  - Limit the validity range of the EFT to the perturbative region. Consider it as a useful parameterization of slight deviations from the SM in the range under the TeV scale.
  - Take advantage of the analytical properties of the S-Matrix (encoded inside dispersion relations and unitarization procedures) to study the non-perturbative region (TeV scale) of the theory.

EFTs + Unitarization Procedures

- We are interested in the collider phenomenology of Vector Bosons Scattering ($WZ \to WZ$), since it is very sensitive to new physics in the EW sector in the LHC.
- Bottom to Top approach: we construct an EFT for the EW sector. $SU(2)_L \times SU(2)_R$, EChL copy of ChPT in QCD.
- Degrees of freedom: Gauge Bosons $W^{\pm}$, Z + Higgs-like particle (h).
- 4 considered parameters: a, $b = a^2$, a_4, a_5.
- The NLO-computed EFT grows with the CM energy like $A \sim s^2$. Hence, it will eventually reach the unitarity bound, becoming non-perturbative. Options:
  - Limit the validity range of the EFT to the perturbative region. Consider it as a useful parameterization of slight deviations from the SM in the range under the TeV scale.
  - Take advantage of the analytical properties of the S-Matrix (encoded inside dispersion relations and unitarization procedures) to study the non-perturbative region (TeV scale) of the theory.

EFTs + Unitarization Procedures

- We are interested in the collider phenomenology of Vector Bosons Scattering ($WZ \to WZ$), since it is very sensitive to new physics in the EW sector in the LHC.
- Bottom to Top approach: we construct an EFT for the EW sector. $SU(2)_L \times SU(2)_R$, EChL copy of ChPT in QCD.
- Degrees of freedom: Gauge Bosons $W^{\pm}$, Z + Higgs-like particle (h).
- 4 considered parameters: a, $b = a^2$, a_4, a_5.
- The NLO-computed EFT grows with the CM energy like $A \sim s^2$. Hence, it will eventually reach the unitarity bound, becoming non-perturbative. Options:
    - Limit the validity range of the EFT to the perturbative region. Consider it as a useful parameterization of slight deviations from the SM in the range under the TeV scale.
    - Take advantage of the analytical properties of the S-Matrix (encoded inside dispersion relations and unitarization procedures) to study the non-perturbative region (TeV scale) of the theory.

EFTs + Unitarization Procedures

- We are interested in the collider phenomenology of Vector Bosons Scattering ($WZ \to WZ$), since it is very sensitive to new physics in the EW sector in the LHC.
- Bottom to Top approach: we construct an EFT for the EW sector. $SU(2)_L \times SU(2)_R$, EChL copy of ChPT in QCD.
- Degrees of freedom: Gauge Bosons $W^{\pm}$, Z + Higgs-like particle (h).
- 4 considered parameters: a, $b = a^2$, a_4, a_5.
- The NLO-computed EFT grows with the CM energy like $A \sim s^2$. Hence, it will eventually reach the unitarity bound, becoming non-perturbative. Options:
    - Limit the validity range of the EFT to the perturbative region. Consider it as a useful parameterization of slight deviations from the SM in the range under the TeV scale.
    - Take advantage of the analytical properties of the S-Matrix (encoded inside dispersion relations and unitarization procedures) to study the non-perturbative region (TeV scale) of the theory.

The naive K-matrix Unit. Method on trouble

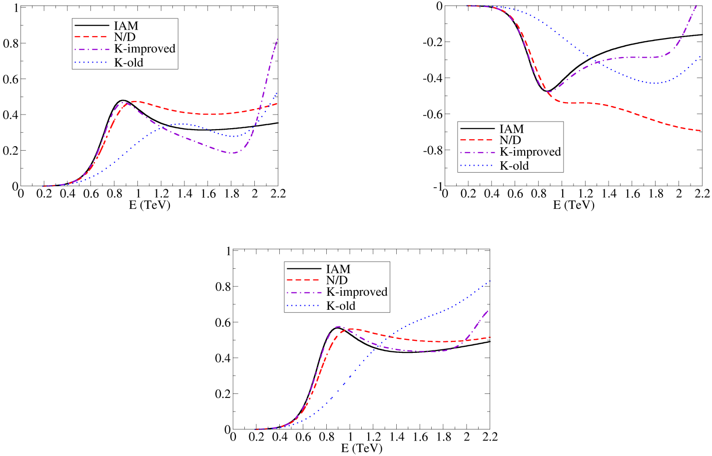

From left to right and top to bottom, elastic $\omega\omega$, elastic hh, and cross channel $\omega\omega \to hh$. $IJ = 00$. $a = 0.88$, $b = 3$, $\mu = 3\,\mathrm{TeV}$ and all NLO parameters set to 0.
PRL **114** (2015) 221803, PRD **91** (2015) 075017.

Reson. in $W_L W_L \to W_L W_L$ due to a_4 and a_5, ours

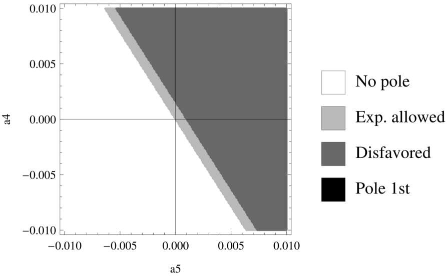

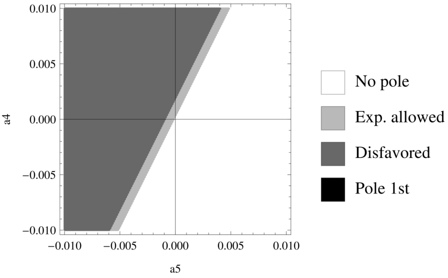

- $a = 0.90$, $b = a^2$
  PRD **91** (2015) 075017
- From left, clockwise,
  $IJ = 00, 11, 20$
- Excluding resonances
  $M_S < 700\,\mathrm{GeV}$, $M_V < 1.5\,\mathrm{TeV}$

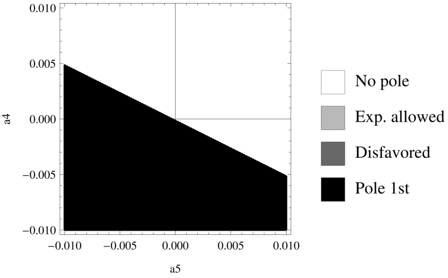

CROSS-CHECK: Espriu, Yencho, Mescia
PRD**88**, 055002
PRD**90**, 015035
At right, exclusion regions include resonances with $M_{S,V} < 600\,\mathrm{GeV}$.

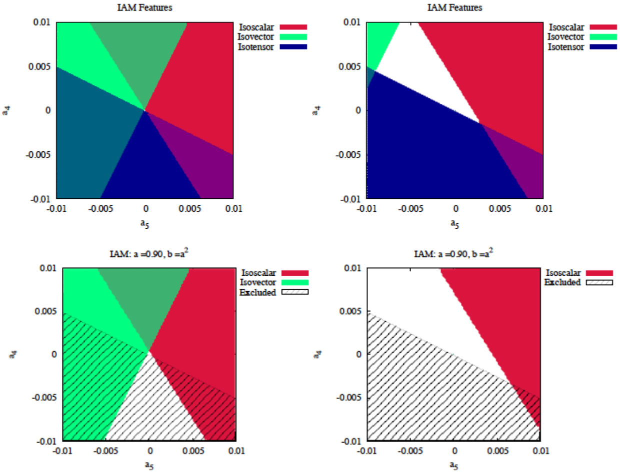

Experimental bounds on low-energy constants

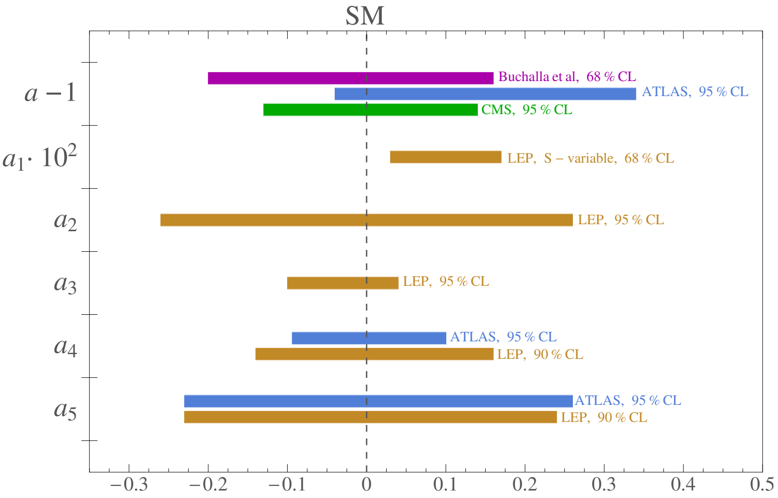

[arXiv:1707.04580 [hep-ph]]

Experimental bounds on low-energy constants, NLO a_4-a_5

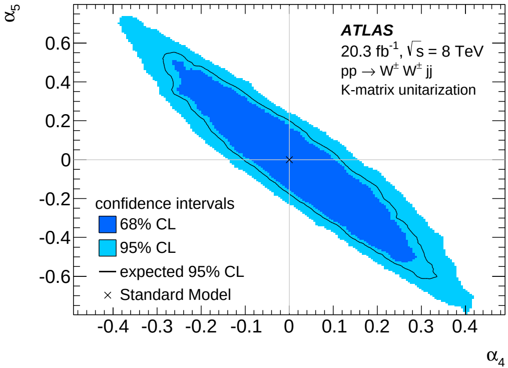

Direct constraint over a_4-a_5 from ATLAS, [PRL**113** (2014) 141803]. Note that the naive K-matrix unitarization procedure from Kilian et al [JHEP 0811, 010] is used here.

A custom model for MadGraph v5

$pp \to WZj_1j_2$

by $WZ \to WZ$ scattering

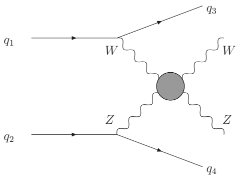

- We are interested in $WZ \to WZ$. Isovector channel ($IJ = 11$).
- The Inverse Amplitude Method (IAM) is used. We do not use the ET in this study, i.e., we consider gauge bosons W and Z in the external legs.
- We couple with initial pp collider states via MadGraph v5 [arXiv:1707.04580 [hep-ph]]. Final states: $WZjj$ or $l_1^+ l_1^- l_2^+ \nu jj$.
- We use a Proca 4-vector formalism to obtain an effective theory that MadGraph can process. Proca paramenters are computed from the original EFT ones. No additional parameters needed.

A custom model for MadGraph v5

$pp \to WZj_1j_2$

by $WZ \to WZ$ scattering

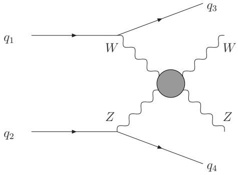

- We are interested in $WZ \to WZ$. Isovector channel ($IJ = 11$).
- The Inverse Amplitude Method (IAM) is used. We do not use the ET in this study, i.e., we consider gauge bosons W and Z in the external legs.
- We couple with initial pp collider states via MadGraph v5 [arXiv:1707.04580 [hep-ph]]. Final states: $WZjj$ or $l_1^+ l_1^- l_2^+ \nu jj$.
- We use a Proca 4-vector formalism to obtain an effective theory that MadGraph can process. Proca paramenters are computed from the original EFT ones. No additional parameters needed.

A custom model for MadGraph v5

$pp \to WZ j_1 j_2$

by $WZ \to WZ$ scattering

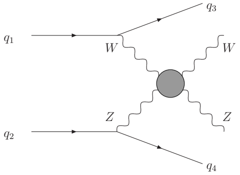

- We are interested in $WZ \to WZ$. Isovector channel ($IJ = 11$).
- The Inverse Amplitude Method (IAM) is used. We do not use the ET in this study, i.e., we consider gauge bosons W and Z in the external legs.
- We couple with initial pp collider states via MadGraph v5 [arXiv:1707.04580 [hep-ph]]. Final states: $WZjj$ or $l_1^+ l_1^- l_2^+ \nu jj$.
- We use a Proca 4-vector formalism to obtain an effective theory that MadGraph can process. Proca paramenters are computed from the original EFT ones. No additional parameters needed.

A custom model for MadGraph v5

$pp \to WZj_1j_2$

by $WZ \to WZ$ scattering

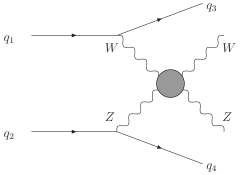

- We are interested in $WZ \to WZ$. Isovector channel ($IJ = 11$).
- The Inverse Amplitude Method (IAM) is used. We do not use the ET in this study, i.e., we consider gauge bosons W and Z in the external legs.
- We couple with initial pp collider states via MadGraph v5 [arXiv:1707.04580 [hep-ph]]. Final states: $WZjj$ or $l_1^+ l_1^- l_2^+ \nu jj$.
- We use a Proca 4-vector formalism to obtain an effective theory that MadGraph can process. Proca paramenters are computed from the original EFT ones. No additional parameters needed.

Isovector Resonance

arXiv:1707.04580 [hep-ph]

BP	$M_V(\mathrm{GeV})$	$\Gamma_V(\mathrm{GeV})$	$g_V(M_V^2)$	a	$a_4 \cdot 10^4$	$a_5 \cdot 10^4$
BP1	1476	14	0.033	1	3.5	-3
BP2	2039	21	0.018	1	1	-1
BP3	2472	27	0.013	1	0.5	-0.5
BP1'	1479	42	0.058	0.9	9.5	-6.5
BP2'	1980	97	0.042	0.9	5.5	-2.5
BP3'	2480	183	0.033	0.9	4	-1

These BPs have been selected for vector resonances emerging at mass and width values that are of phenomenological interest for the LHC.
Considered backgrounds: The pure SM-EW background, of order $\mathcal{O}(\alpha_{\mathrm{em}}^2)$.
The mixed SM-QCDEW background, of order $\mathcal{O}(\alpha_{\mathrm{em}}\alpha_s)$.

Isovector Resonance: *WZ* in final state

arXiv:1707.04580 [hep-ph]

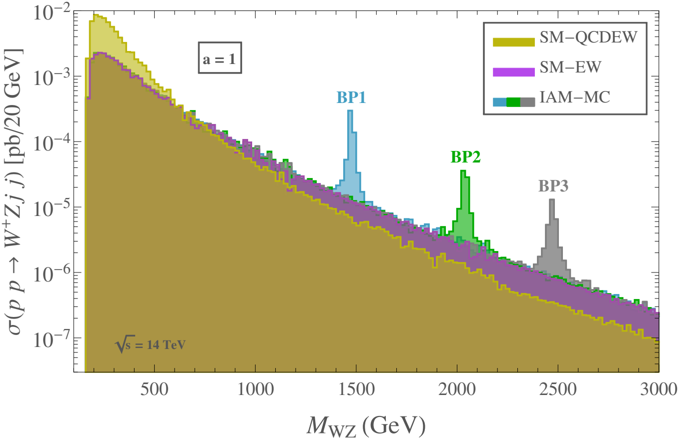

$a = 1$; $a_4 \cdot 10^4 = 3.5$ (BP1), 1 (BP2), 0.5 (BP3);

$-a_5 \cdot 10^4 = 3$ (BP1), 1 (BP2), 0.5 (BP3).

Isovector Resonance: leptonic final state

arXiv:1707.04580 [hep-ph]

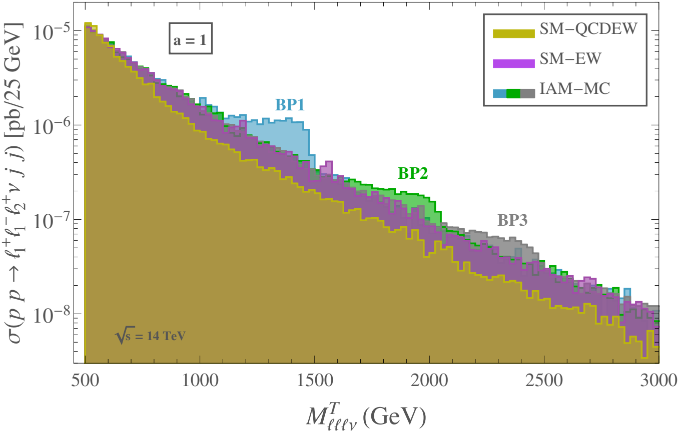

$a = 1$; $a_4 \cdot 10^4 = 3.5$ (BP1), 1 (BP2), 0.5 (BP3);

$-a_5 \cdot 10^4 = 3$ (BP1), 1 (BP2), 0.5 (BP3).

Isovector Resonance: *WZ* in final state

arXiv:1707.04580 [hep-ph]

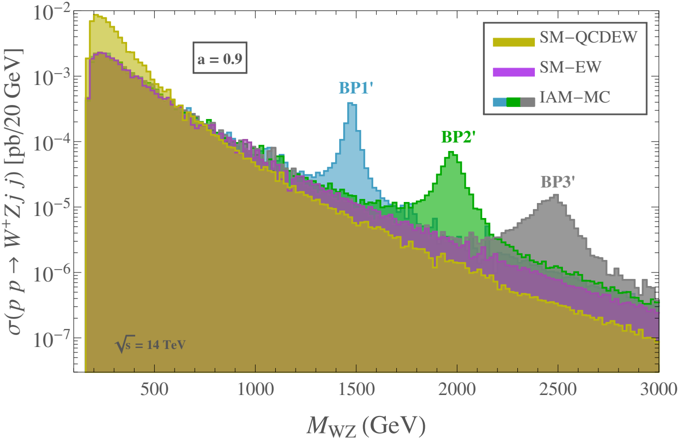

$a = 0.9$; $a_4 \cdot 10^4 = 3.5$ (BP1'), 1 (BP2'), 0.5 (BP3');

$-a_5 \cdot 10^4 = 3$ (BP1'), 1 (BP2'), 0.5 (BP3').

Isovector Resonance: leptonic final state

arXiv:1707.04580 [hep-ph]

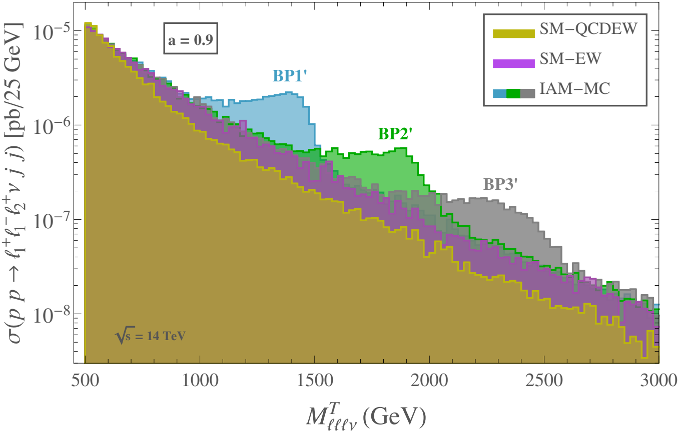

$a = 0.9$; $a_4 \cdot 10^4 = 3.5$ (BP1'), 1 (BP2'), 0.5 (BP3');

$-a_5 \cdot 10^4 = 3$ (BP1'), 1 (BP2'), 0.5 (BP3').

Conclusions

- Studied $2 \to 2$ scattering processes within the EWSBS: $WZ \to WZ$.
- We provide a MadGraph v5 model for the unitarized EChL, without relying on the naive K-matrix.
- We are able to reproduce collider signals, as required by experimentalists.
- We present realistic predictions of $(lll\nu jj)$ events at LHC from V resonance production via WZ scat. and compare with backgs.
- Prospects for the Benchmark Points at the LHC ($14\,\mathrm{TeV}$):

	$\mathcal{L} = 300\,\mathrm{fb}^{-1}$			$\mathcal{L} = 1000\,\mathrm{fb}^{-1}$			$\mathcal{L} = 3000\,\mathrm{fb}^{-1}$		
	N_l^{IAM}	N_l^{SM}	σ_l^{stat}	N_l^{IAM}	N_l^{SM}	σ_l^{stat}	N_l^{IAM}	N_l^{SM}	σ_l^{stat}
BP1	2	1	0.6	6	4	1.1	19	13	1.8
BP2	0.6	0.4	-	1	1	0	4	3	0.1
BP3	0.1	0.1	-	0.4	0.3	-	1	1	0
BP1'	6	2	2.3	19	8	4.2	57	23	7.2
BP2'	2	0.9	1	6	3	1.8	19	9	3.7
BP3'	0.8	0.4	-	3	1	1.1	8	4	1.8

Conclusions

- Studied $2 \to 2$ scattering processes within the EWSBS: $WZ \to WZ$.
- We provide a MadGraph v5 model for the unitarized EChL, without relying on the naive K-matrix.
- We are able to reproduce collider signals, as required by experimentalists.
- We present realistic predictions of $(lll\nu jj)$ events at LHC from V resonance production via WZ scat. and compare with backgs.
- Prospects for the Benchmark Points at the LHC (14 TeV):

	$\mathcal{L} = 300\,\mathrm{fb}^{-1}$			$\mathcal{L} = 1000\,\mathrm{fb}^{-1}$			$\mathcal{L} = 3000\,\mathrm{fb}^{-1}$		
	N_l^{IAM}	N_l^{SM}	σ_l^{stat}	N_l^{IAM}	N_l^{SM}	σ_l^{stat}	N_l^{IAM}	N_l^{SM}	σ_l^{stat}
BP1	2	1	0.6	6	4	1.1	19	13	1.8
BP2	0.6	0.4	-	1	1	0	4	3	0.1
BP3	0.1	0.1	-	0.4	0.3	-	1	1	0
BP1'	6	2	2.3	19	8	4.2	57	23	7.2
BP2'	2	0.9	1	6	3	1.8	19	9	3.7
BP3'	0.8	0.4	-	3	1	1.1	8	4	1.8

Conclusions

- Studied $2 \to 2$ scattering processes within the EWSBS: $WZ \to WZ$.
- We provide a MadGraph v5 model for the unitarized EChL, without relying on the naive K-matrix.
- We are able to reproduce collider signals, as required by experimentalists.
- We present realistic predictions of $(lll\nu jj)$ events at LHC from V resonance production via WZ scat. and compare with backgs.
- Prospects for the Benchmark Points at the LHC (14 TeV):

	$\mathcal{L} = 300\,\mathrm{fb}^{-1}$			$\mathcal{L} = 1000\,\mathrm{fb}^{-1}$			$\mathcal{L} = 3000\,\mathrm{fb}^{-1}$		
	N_l^{IAM}	N_l^{SM}	σ_l^{stat}	N_l^{IAM}	N_l^{SM}	σ_l^{stat}	N_l^{IAM}	N_l^{SM}	σ_l^{stat}
BP1	2	1	0.6	6	4	1.1	19	13	1.8
BP2	0.6	0.4	-	1	1	0	4	3	0.1
BP3	0.1	0.1	-	0.4	0.3	-	1	1	0
BP1'	6	2	2.3	19	8	4.2	57	23	7.2
BP2'	2	0.9	1	6	3	1.8	19	9	3.7
BP3'	0.8	0.4	-	3	1	1.1	8	4	1.8

Conclusions

- Studied $2 \to 2$ scattering processes within the EWSBS: $WZ \to WZ$.
- We provide a MadGraph v5 model for the unitarized EChL, without relying on the naive K-matrix.
- We are able to reproduce collider signals, as required by experimentalists.
- We present realistic predictions of $(lll\nu jj)$ events at LHC from V resonance production via WZ scat. and compare with backgs.
- Prospects for the Benchmark Points at the LHC (14 TeV):

	$\mathcal{L} = 300\,\text{fb}^{-1}$			$\mathcal{L} = 1000\,\text{fb}^{-1}$			$\mathcal{L} = 3000\,\text{fb}^{-1}$		
	N_l^{IAM}	N_l^{SM}	σ_l^{stat}	N_l^{IAM}	N_l^{SM}	σ_l^{stat}	N_l^{IAM}	N_l^{SM}	σ_l^{stat}
BP1	2	1	0.6	6	4	1.1	19	13	1.8
BP2	0.6	0.4	-	1	1	0	4	3	0.1
BP3	0.1	0.1	-	0.4	0.3	-	1	1	0
BP1'	6	2	2.3	19	8	4.2	57	23	7.2
BP2'	2	0.9	1	6	3	1.8	19	9	3.7
BP3'	0.8	0.4	-	3	1	1.1	8	4	1.8

Conclusions

- Studied $2 \to 2$ scattering processes within the EWSBS: $WZ \to WZ$.
- We provide a MadGraph v5 model for the unitarized EChL, without relying on the naive K-matrix.
- We are able to reproduce collider signals, as required by experimentalists.
- We present realistic predictions of $(lll\nu jj)$ events at LHC from V resonance production via WZ scat. and compare with backgs.
- Prospects for the Benchmark Points at the LHC ($14\,\mathrm{TeV}$):

	$\mathcal{L} = 300\,\mathrm{fb}^{-1}$			$\mathcal{L} = 1000\,\mathrm{fb}^{-1}$			$\mathcal{L} = 3000\,\mathrm{fb}^{-1}$		
	$N_l^{\rm IAM}$	$N_l^{\rm SM}$	$\sigma_l^{\rm stat}$	$N_l^{\rm IAM}$	$N_l^{\rm SM}$	$\sigma_l^{\rm stat}$	$N_l^{\rm IAM}$	$N_l^{\rm SM}$	$\sigma_l^{\rm stat}$
BP1	2	1	0.6	6	4	1.1	19	13	1.8
BP2	0.6	0.4	-	1	1	0	4	3	0.1
BP3	0.1	0.1	-	0.4	0.3	-	1	1	0
BP1'	6	2	2.3	19	8	4.2	57	23	7.2
BP2'	2	0.9	1	6	3	1.8	19	9	3.7
BP3'	0.8	0.4	-	3	1	1.1	8	4	1.8

Conclusions

- With $300\,\mathrm{fb}^{-1}$, a first hint (with $\sigma_l^{\mathrm{stat}} > 2$) of resonances with mass around 1.5 TeV for $a \neq 1$ could be seen.
- With $1000\,\mathrm{fb}^{-1}$, we estimate that these type of resonances could be observed with $\sigma_l^{\mathrm{stat}} > 4$ and new hints of the heavier resonances with masses close to $2\,\mathrm{TeV}$ could also appear.
- All these resonances with masses below $2\,\mathrm{TeV}$ could be seen with $3000\,\mathrm{fb}^{-1}$.
- A fully efficient study of charged vector resonances with masses heavier than $2\,\mathrm{TeV}$ would imply to analyze also the semileptonic and the hadronic decay channels of the *WZ* final gauge bosons.
- We are ready for strong interactions. What happens in nature?
  - SM → unitarity.
  - Higgsless model (now experimentally excluded) → unitarity violation in *WW* scattering → new physics.
  - Higgs–like boson found → no unitarity violation?
  - Depends on couplings. Ok with the present experimental bounds.
  - Let us wait for the LHC data.

Conclusions

- With 300 fb^{-1}, a first hint (with $\sigma_l^{\mathrm{stat}} > 2$) of resonances with mass around 1.5 TeV for $a \neq 1$ could be seen.
- With 1000 fb^{-1}, we estimate that these type of resonances could be observed with $\sigma_l^{\mathrm{stat}} > 4$ and new hints of the heavier resonances with masses close to 2 TeV could also appear.
- All these resonances with masses below 2 TeV could be seen with 3000 fb^{-1}.
- A fully efficient study of charged vector resonances with masses heavier than 2 TeV would imply to analyze also the semileptonic and the hadronic decay channels of the WZ final gauge bosons.
- We are ready for strong interactions. What happens in nature?
  - SM $\to$ unitarity.
  - Higgsless model (now experimentally excluded) $\to$ unitarity violation in WW scattering $\to$ new physics.
  - Higgs–like boson found $\to$ no unitarity violation?
  - Depends on couplings. Ok with the present experimental bounds.
  - Let us wait for the LHC data.

Conclusions

- With $300\,\mathrm{fb}^{-1}$, a first hint (with $\sigma_I^{\mathrm{stat}} > 2$) of resonances with mass around 1.5 TeV for $a \neq 1$ could be seen.
- With $1000\,\mathrm{fb}^{-1}$, we estimate that these type of resonances could be observed with $\sigma_I^{\mathrm{stat}} > 4$ and new hints of the heavier resonances with masses close to $2\,\mathrm{TeV}$ could also appear.
- All these resonances with masses below $2\,\mathrm{TeV}$ could be seen with $3000\,\mathrm{fb}^{-1}$.
- A fully efficient study of charged vector resonances with masses heavier than $2\,\mathrm{TeV}$ would imply to analyze also the semileptonic and the hadronic decay channels of the WZ final gauge bosons.
- We are ready for strong interactions. What happens in nature?
  - SM $\to$ unitarity.
  - Higgsless model (now experimentally excluded) $\to$ unitarity violation in WW scattering $\to$ new physics.
  - Higgs–like boson found $\to$ no unitarity violation?
  - Depends on couplings. Ok with the present experimental bounds.
  - Let us wait for the LHC data.

Conclusions

- With $300\,\mathrm{fb}^{-1}$, a first hint (with $\sigma_l^{\mathrm{stat}} > 2$) of resonances with mass around 1.5 TeV for $a \neq 1$ could be seen.
- With $1000\,\mathrm{fb}^{-1}$, we estimate that these type of resonances could be observed with $\sigma_l^{\mathrm{stat}} > 4$ and new hints of the heavier resonances with masses close to $2\,\mathrm{TeV}$ could also appear.
- All these resonances with masses below $2\,\mathrm{TeV}$ could be seen with $3000\,\mathrm{fb}^{-1}$.
- A fully efficient study of charged vector resonances with masses heavier than $2\,\mathrm{TeV}$ would imply to analyze also the semileptonic and the hadronic decay channels of the WZ final gauge bosons.
- We are ready for strong interactions. What happens in nature?
  - SM $\to$ unitarity.
  - Higgsless model (now experimentally excluded) $\to$ unitarity violation in WW scattering $\to$ new physics.
  - Higgs–like boson found $\to$ no unitarity violation?
  - Depends on couplings. Ok with the present experimental bounds.
  - Let us wait for the LHC data.

Conclusions

- With $300\,\mathrm{fb}^{-1}$, a first hint (with $\sigma_I^{\mathrm{stat}} > 2$) of resonances with mass around 1.5 TeV for $a \neq 1$ could be seen.
- With $1000\,\mathrm{fb}^{-1}$, we estimate that these type of resonances could be observed with $\sigma_I^{\mathrm{stat}} > 4$ and new hints of the heavier resonances with masses close to $2\,\mathrm{TeV}$ could also appear.
- All these resonances with masses below $2\,\mathrm{TeV}$ could be seen with $3000\,\mathrm{fb}^{-1}$.
- A fully efficient study of charged vector resonances with masses heavier than $2\,\mathrm{TeV}$ would imply to analyze also the semileptonic and the hadronic decay channels of the WZ final gauge bosons.
- We are ready for strong interactions. What happens in nature?
  - SM $\to$ unitarity.
  - Higgsless model (now experimentally excluded) $\to$ unitarity violation in WW scattering $\to$ new physics.
  - Higgs–like boson found $\to$ no unitarity violation?
  - Depends on couplings. Ok with the present experimental bounds.
  - Let us wait for the LHC data.

Conclusions

- With $300\,\mathrm{fb}^{-1}$, a first hint (with $\sigma_I^{\mathrm{stat}} > 2$) of resonances with mass around 1.5 TeV for $a \neq 1$ could be seen.
- With $1000\,\mathrm{fb}^{-1}$, we estimate that these type of resonances could be observed with $\sigma_I^{\mathrm{stat}} > 4$ and new hints of the heavier resonances with masses close to $2\,\mathrm{TeV}$ could also appear.
- All these resonances with masses below $2\,\mathrm{TeV}$ could be seen with $3000\,\mathrm{fb}^{-1}$.
- A fully efficient study of charged vector resonances with masses heavier than $2\,\mathrm{TeV}$ would imply to analyze also the semileptonic and the hadronic decay channels of the WZ final gauge bosons.
- We are ready for strong interactions. What happens in nature?
  - SM $\rightarrow$ unitarity.
  - Higgsless model (now experimentally excluded) $\rightarrow$ unitarity violation in WW scattering $\rightarrow$ new physics.
  - Higgs–like boson found $\rightarrow$ no unitarity violation?
  - Depends on couplings. Ok with the present experimental bounds.
  - Let us wait for the LHC data.

Conclusions

- With $300\,\mathrm{fb}^{-1}$, a first hint (with $\sigma_I^{\mathrm{stat}} > 2$) of resonances with mass around 1.5 TeV for $a \neq 1$ could be seen.
- With $1000\,\mathrm{fb}^{-1}$, we estimate that these type of resonances could be observed with $\sigma_I^{\mathrm{stat}} > 4$ and new hints of the heavier resonances with masses close to $2\,\mathrm{TeV}$ could also appear.
- All these resonances with masses below $2\,\mathrm{TeV}$ could be seen with $3000\,\mathrm{fb}^{-1}$.
- A fully efficient study of charged vector resonances with masses heavier than $2\,\mathrm{TeV}$ would imply to analyze also the semileptonic and the hadronic decay channels of the *WZ* final gauge bosons.
- We are ready for strong interactions. What happens in nature?
  - SM $\rightarrow$ unitarity.
  - Higgsless model (now experimentally excluded) $\rightarrow$ unitarity violation in *WW* scattering $\rightarrow$ new physics.
  - Higgs–like boson found $\rightarrow$ no unitarity violation?
  - Depends on couplings. Ok with the present experimental bounds.
  - Let us wait for the LHC data.

Conclusions

- With $300\,\mathrm{fb}^{-1}$, a first hint (with $\sigma_I^{\mathrm{stat}} > 2$) of resonances with mass around 1.5 TeV for $a \neq 1$ could be seen.
- With $1000\,\mathrm{fb}^{-1}$, we estimate that these type of resonances could be observed with $\sigma_I^{\mathrm{stat}} > 4$ and new hints of the heavier resonances with masses close to $2\,\mathrm{TeV}$ could also appear.
- All these resonances with masses below $2\,\mathrm{TeV}$ could be seen with $3000\,\mathrm{fb}^{-1}$.
- A fully efficient study of charged vector resonances with masses heavier than $2\,\mathrm{TeV}$ would imply to analyze also the semileptonic and the hadronic decay channels of the WZ final gauge bosons.
- We are ready for strong interactions. What happens in nature?
  - SM $\rightarrow$ unitarity.
  - Higgsless model (now experimentally excluded) $\rightarrow$ unitarity violation in WW scattering $\rightarrow$ new physics.
  - Higgs–like boson found $\rightarrow$ no unitarity violation?
  - Depends on couplings. Ok with the present experimental bounds.
  - Let us wait for the LHC data.

Conclusions

- With $300\,\mathrm{fb}^{-1}$, a first hint (with $\sigma_I^{\rm stat} > 2$) of resonances with mass around 1.5 TeV for $a \neq 1$ could be seen.
- With $1000\,\mathrm{fb}^{-1}$, we estimate that these type of resonances could be observed with $\sigma_I^{\rm stat} > 4$ and new hints of the heavier resonances with masses close to $2\,\mathrm{TeV}$ could also appear.
- All these resonances with masses below $2\,\mathrm{TeV}$ could be seen with $3000\,\mathrm{fb}^{-1}$.
- A fully efficient study of charged vector resonances with masses heavier than $2\,\mathrm{TeV}$ would imply to analyze also the semileptonic and the hadronic decay channels of the *WZ* final gauge bosons.
- We are ready for strong interactions. What happens in nature?
  - SM $\rightarrow$ unitarity.
  - Higgsless model (now experimentally excluded) $\rightarrow$ unitarity violation in *WW* scattering $\rightarrow$ new physics.
  - Higgs–like boson found $\rightarrow$ no unitarity violation?
  - Depends on couplings. Ok with the present experimental bounds.
  - Let us wait for the LHC data.

Conclusions

- With $300\,\mathrm{fb}^{-1}$, a first hint (with $\sigma_I^{\mathrm{stat}} > 2$) of resonances with mass around 1.5 TeV for $a \neq 1$ could be seen.
- With $1000\,\mathrm{fb}^{-1}$, we estimate that these type of resonances could be observed with $\sigma_I^{\mathrm{stat}} > 4$ and new hints of the heavier resonances with masses close to $2\,\mathrm{TeV}$ could also appear.
- All these resonances with masses below $2\,\mathrm{TeV}$ could be seen with $3000\,\mathrm{fb}^{-1}$.
- A fully efficient study of charged vector resonances with masses heavier than $2\,\mathrm{TeV}$ would imply to analyze also the semileptonic and the hadronic decay channels of the WZ final gauge bosons.
- We are ready for strong interactions. What happens in nature?
  - SM $\rightarrow$ unitarity.
  - Higgsless model (now experimentally excluded) $\rightarrow$ unitarity violation in WW scattering $\rightarrow$ new physics.
  - Higgs–like boson found $\rightarrow$ no unitarity violation?
  - Depends on couplings. Ok with the present experimental bounds.
  - Let us wait for the LHC data.

Backup Slides

Empirical situation: $\gamma\gamma$ physics

- Current efforts to measure $\gamma\gamma \to W_L^+ W_L^-$ and $\gamma\gamma \to Z_L Z_L$ channels.
- Only 2 events measured. Graphs from CMS[1].
- Wait for LHC Run–II, CMS–TOTEM and ATLAS–AFP.
- Efforts for measuring $\gamma\gamma$ final states: SM Higgs decay channel.

[1] JHEP **07** (2013) 116

Empirical situation: $\gamma\gamma$ physics

- Current efforts to measure $\gamma\gamma \to W_L^+ W_L^-$ and $\gamma\gamma \to Z_L Z_L$ channels.
- Only 2 events measured. Graphs from CMS[1].
- Wait for LHC Run–II, CMS–TOTEM and ATLAS–AFP.
- Efforts for measuring $\gamma\gamma$ final states: SM Higgs decay channel.

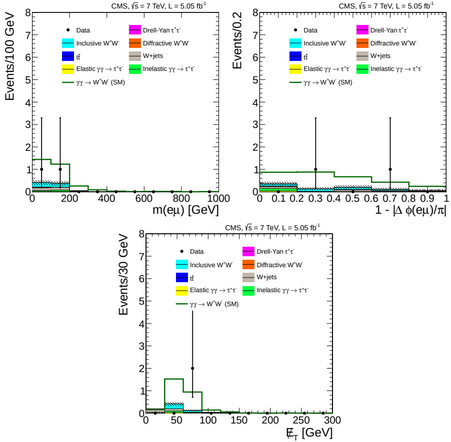

[1] JHEP **07** (2013) 116

- Current efforts to measure $\gamma\gamma \to W_L^+ W_L^-$ and $\gamma\gamma \to Z_L Z_L$ channels.
- Only 2 events measured. Graphs from CMS[1].
- Wait for LHC Run–II, CMS–TOTEM and ATLAS–AFP.
- Efforts for measuring $\gamma\gamma$ final states: SM Higgs decay channel.

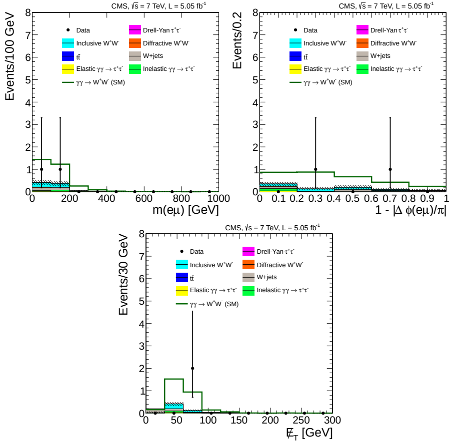

[1] JHEP **07** (2013) 116

- Current efforts to measure $\gamma\gamma \to W_L^+ W_L^-$ and $\gamma\gamma \to Z_L Z_L$ channels.
- Only 2 events measured. Graphs from CMS[1].
- Wait for LHC Run–II, CMS–TOTEM and ATLAS–AFP.
- Efforts for measuring $\gamma\gamma$ final states: SM Higgs decay channel.

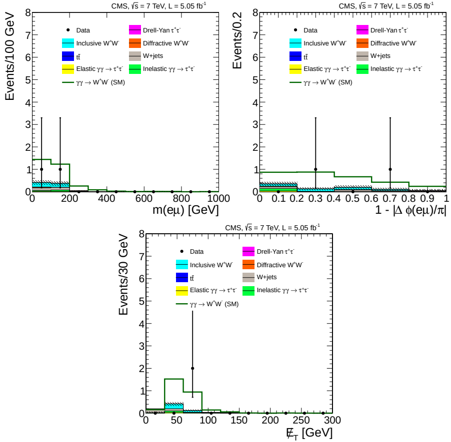

[1] JHEP **07** (2013) 116

Empirical situation: $t\bar{t}$ physics

- Initial $t\bar{t}$ states are important because of gluon fusion processes, with a large cross section at the LHC.
- The production of $t\bar{t}$ states is also a well studied experimental observable at the LHC.

Top quark loop in the SM: VV states from gluon fusion

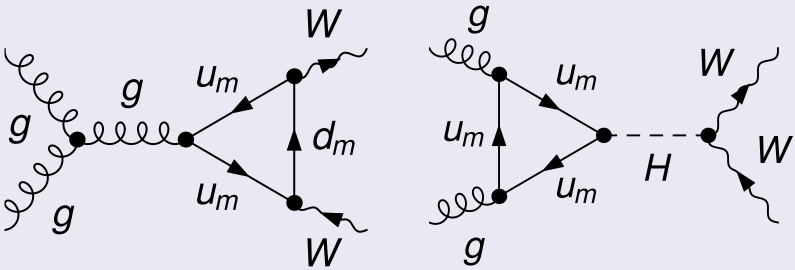

Empirical situation: $t\bar{t}$ physics

- Initial $t\bar{t}$ states are important because of gluon fusion processes, with a large cross section at the LHC.
- The production of $t\bar{t}$ states is also a well studied experimental observable at the LHC.

Top quark loop in the SM: VV states from gluon fusion

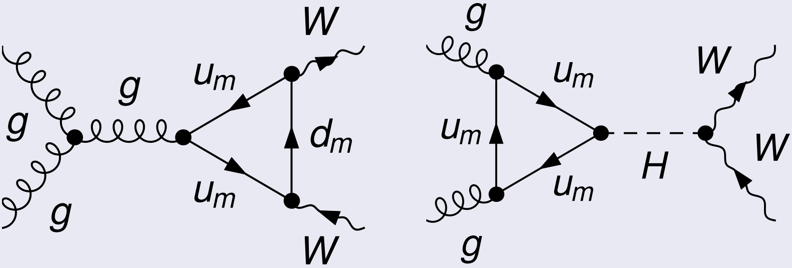

Studied framework

- We consider a strongly interacting EWSBS, in contrast to the weakly interacting one of the SM.
- We study the processes $VV \to VV$, $VV \to hh$ and $hh \to hh$, and extend the result to include $\gamma\gamma$ and $t\bar{t}$ states.
- Our LO scattering amplitudes within the EWSBS diverge, but are controlled by strongly interacting dynamics which respect unitarity. This situation is similar to low-energy QCD (hadron physics).
- In order to minimize our assumptions over the (hypothetical) underlying theory, we will
  - use dispersion relations over a partial wave decomposition (the so–called unitarization procedures);
  - extend these unitarization procedures to the coupled-channels case;
  - and consider an Effective Field Theory, computed at the NLO level (within the limits of the Equivalence Theorem), with three would-be Goldstone bosons ω and a Higgs-like boson h.

Studied framework

- We consider a strongly interacting EWSBS, in contrast to the weakly interacting one of the SM.
- We study the processes $VV \to VV$, $VV \to hh$ and $hh \to hh$, and extend the result to include $\gamma\gamma$ and $t\bar{t}$ states.
- Our LO scattering amplitudes within the EWSBS diverge, but are controlled by strongly interacting dynamics which respect unitarity. This situation is similar to low-energy QCD (hadron physics).
- In order to minimize our assumptions over the (hypothetical) underlying theory, we will
  - use dispersion relations over a partial wave decomposition (the so-called unitarization procedures);
  - extend these unitarization procedures to the coupled-channels case;
  - and consider an Effective Field Theory, computed at the NLO level (within the limits of the Equivalence Theorem), with three would-be Goldstone bosons ω and a Higgs-like boson h.

Studied framework

- We consider a strongly interacting EWSBS, in contrast to the weakly interacting one of the SM.
- We study the processes $VV \to VV$, $VV \to hh$ and $hh \to hh$, and extend the result to include $\gamma\gamma$ and $t\bar{t}$ states.
- Our LO scattering amplitudes within the EWSBS diverge, but are controlled by strongly interacting dynamics which respect unitarity. This situation is similar to low-energy QCD (hadron physics).
- In order to minimize our assumptions over the (hypothetical) underlying theory, we will
  - use dispersion relations over a partial wave decomposition (the so-called unitarization procedures).
  - extend these unitarization procedures to the coupled-channels case;
  - and consider an Effective Field Theory, computed at the NLO level (within the limits of the Equivalence Theorem), with three would-be Goldstone bosons ω and a Higgs-like boson h.

Studied framework

- We consider a strongly interacting EWSBS, in contrast to the weakly interacting one of the SM.
- We study the processes $VV \to VV$, $VV \to hh$ and $hh \to hh$, and extend the result to include $\gamma\gamma$ and $t\bar{t}$ states.
- Our LO scattering amplitudes within the EWSBS diverge, but are controlled by strongly interacting dynamics which respect unitarity. This situation is similar to low-energy QCD (hadron physics).
- In order to minimize our assumptions over the (hypothetical) underlying theory, we will
  - use dispersion relations over a partial wave decomposition (the so–called unitarization procedures);
  - extend these unitarization procedures to the coupled-channels case;
  - and consider an Effective Field Theory, computed at the NLO level (within the limits of the Equivalence Theorem), with three would-be Goldstone bosons ω and a Higgs-like boson h.

Studied framework

- We consider a strongly interacting EWSBS, in contrast to the weakly interacting one of the SM.
- We study the processes $VV \to VV$, $VV \to hh$ and $hh \to hh$, and extend the result to include $\gamma\gamma$ and $t\bar{t}$ states.
- Our LO scattering amplitudes within the EWSBS diverge, but are controlled by strongly interacting dynamics which respect unitarity. This situation is similar to low-energy QCD (hadron physics).
- In order to minimize our assumptions over the (hypothetical) underlying theory, we will
  - use dispersion relations over a partial wave decomposition (the so–called unitarization procedures);
  - extend these unitarization procedures to the coupled-channels case;
  - and consider an Effective Field Theory, computed at the NLO level (within the limits of the Equivalence Theorem), with three would-be Goldstone bosons ω and a Higgs-like boson h.

Studied framework

- We consider a strongly interacting EWSBS, in contrast to the weakly interacting one of the SM.
- We study the processes $VV \to VV$, $VV \to hh$ and $hh \to hh$, and extend the result to include $\gamma\gamma$ and $t\bar{t}$ states.
- Our LO scattering amplitudes within the EWSBS diverge, but are controlled by strongly interacting dynamics which respect unitarity. This situation is similar to low-energy QCD (hadron physics).
- In order to minimize our assumptions over the (hypothetical) underlying theory, we will
  - use dispersion relations over a partial wave decomposition (the so–called unitarization procedures);
  - extend these unitarization procedures to the coupled-channels case;
  - and consider an Effective Field Theory, computed at the NLO level (within the limits of the Equivalence Theorem), with three would-be Goldstone bosons ω and a Higgs-like boson h.

Studied framework

- We consider a strongly interacting EWSBS, in contrast to the weakly interacting one of the SM.
- We study the processes $VV \to VV$, $VV \to hh$ and $hh \to hh$, and extend the result to include $\gamma\gamma$ and $t\bar{t}$ states.
- Our LO scattering amplitudes within the EWSBS diverge, but are controlled by strongly interacting dynamics which respect unitarity. This situation is similar to low-energy QCD (hadron physics).
- In order to minimize our assumptions over the (hypothetical) underlying theory, we will
  - use dispersion relations over a partial wave decomposition (the so–called unitarization procedures);
  - extend these unitarization procedures to the coupled-channels case;
  - and consider an Effective Field Theory, computed at the NLO level (within the limits of the Equivalence Theorem), with three would-be Goldstone bosons ω and a Higgs-like boson h.

Strongly Interacting Effective Field Theory + Unitarity: similarity with hadronic physics

Chiral Perturbation Theory plus Dispersion Relations.

Simultaneous description of $\pi\pi \to \pi\pi$ and $\pi K \pi K \to \pi K \pi K$ up to 800-1000 MeV including resonances.

Lowest order ChPT (WeinbergTheorems) and even one-loop computations are only valid at very low energies.

A. Dobado and J.R. Peláez: SLAC-PUB-8031, arXiv:9812362v1; Phys. Rev. **D56** (1997) 3057-3073

Strongly Interacting Effective Field Theory + Unitarity: similarity with hadronic physics

Chiral Perturbation Theory plus Dispersion Relations.

Simultaneous description of $\pi\pi \to \pi\pi$ and $\pi K \pi K \to \pi K \pi K$ up to 800-1000 MeV including resonances.

Lowest order ChPT (WeinbergTheorems) and even one-loop computations are only valid at very low energies.

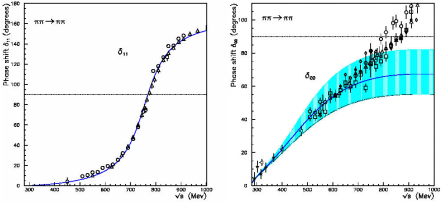

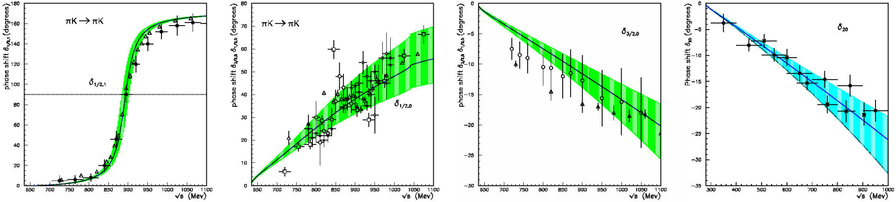

A. Dobado and J.R. Peláez: SLAC-PUB-8031, arXiv:9812362v1; Phys. Rev. **D56** (1997) 3057-3073

Strongly Interacting Effective Field Theory + Unitarity: similarity with hadronic physics

Chiral Perturbation Theory plus Dispersion Relations.

Simultaneous description of $\pi\pi \to \pi\pi$ and $\pi K \pi K \to \pi K \pi K$ up to 800-1000 MeV including resonances.

Lowest order ChPT (WeinbergTheorems) and even one-loop computations are only valid at very low energies.

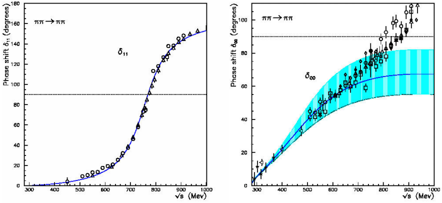

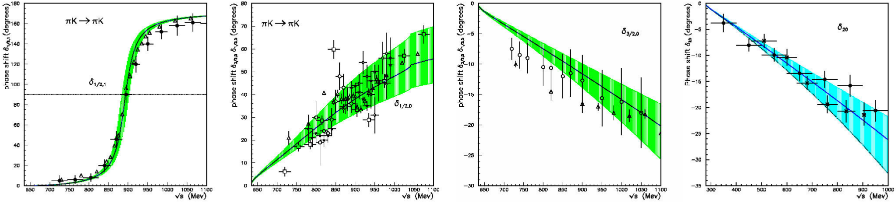

A. Dobado and J.R. Peláez: SLAC-PUB-8031, arXiv:9812362v1; Phys. Rev. **D56** (1997) 3057-3073

Equivalence Theorem

- For $s \gg M_h^2, M_W^2, M_Z^2 \approx (100\,\mathrm{GeV})^2$, longitudinal modes of gauge bosons can be identified with the would-be Goldstones. For instance,

$$T(W_L^a W_L^b \to W_L^c W_L^d) = T(\omega^a \omega^b \to \omega^c \omega^d) + \mathcal{O}\left(M_W/\sqrt{s}\right)$$

- The EWSBS behaves as if the would-be Goldstone bosons were physical states. The non-gauged Lagragian can be used directly to compute scattering amplitudes.
- During the 90's, the limits of applicability of this theorem were studied in detail, leading to the conclusion that it is valid for chiral Lagrangians, like those used in this presentation:

  works from W.B.Kilgore, P.B.Pal, X.Zhang, A.Dobado, J.R.Peláez, M.T.Urdiales, H.-J.He, Y.-P.Kuang, D.Espriu, J.Matias, J.F.Donoghue, J.Tandean,...

Equivalence Theorem

- For $s \gg M_h^2, M_W^2, M_Z^2 \approx (100\,\mathrm{GeV})^2$, longitudinal modes of gauge bosons can be identified with the would-be Goldstones. For instance,

$$T(W_L^a W_L^b \to W_L^c W_L^d) = T(\omega^a \omega^b \to \omega^c \omega^d) + \mathcal{O}\left(M_W/\sqrt{s}\right)$$

- The EWSBS behaves as if the would-be Goldstone bosons were physical states. The non-gauged Lagragian can be used directly to compute scattering amplitudes.
- During the 90's, the limits of applicability of this theorem were studied in detail, leading to the conclusion that it is valid for chiral Lagrangians, like those used in this presentation:

works from W.B.Kilgore, P.B.Pal, X.Zhang, A.Dobado, J.R.Peláez, M.T.Urdiales, H.-J.He, Y.-P.Kuang, D.Espriu, J.Matias, J.F.Donoghue, J.Tandean,...

Equivalence Theorem

- For $s \gg M_h^2, M_W^2, M_Z^2 \approx (100\,\mathrm{GeV})^2$, longitudinal modes of gauge bosons can be identified with the would-be Goldstones. For instance,

$$T(W_L^a W_L^b \to W_L^c W_L^d) = T(\omega^a \omega^b \to \omega^c \omega^d) + \mathcal{O}\left(M_W/\sqrt{s}\right)$$

- The EWSBS behaves as if the would-be Goldstone bosons were physical states. The non-gauged Lagragian can be used directly to compute scattering amplitudes.
- During the 90's, the limits of applicability of this theorem were studied in detail, leading to the conclusion that it is valid for chiral Lagrangians, like those used in this presentation:

  works from W.B.Kilgore, P.B.Pal, X.Zhang, A.Dobado, J.R.Peláez, M.T.Urdiales, H.-J.He, Y.-P.Kuang, D.Espriu, J.Matias, J.F.Donoghue, J.Tandean,...

Equivalence Theorem

- For $s \gg M_h^2, M_W^2, M_Z^2 \approx (100\,\mathrm{GeV})^2$, longitudinal modes of gauge bosons can be identified with the would-be Goldstones. For instance,

$$T(W_L^a W_L^b \to W_L^c W_L^d) = T(\omega^a \omega^b \to \omega^c \omega^d) + \mathcal{O}\left(M_W/\sqrt{s}\right)$$

- The EWSBS behaves as if the would-be Goldstone bosons were physical states. The non-gauged Lagragian can be used directly to compute scattering amplitudes.
- During the 90's, the limits of applicability of this theorem were studied in detail, leading to the conclusion that it is valid for chiral Lagrangians, like those used in this presentation:

works from W.B.Kilgore, P.B.Pal, X.Zhang, A.Dobado, J.R.Peláez, M.T.Urdiales, H.-J.He, Y.-P.Kuang, D.Espriu, J.Matias, J.F.Donoghue, J.Tandean,...

Equivalence Theorem

- For $s \gg M_h^2, M_W^2, M_Z^2 \approx (100\,\mathrm{GeV})^2$, longitudinal modes of gauge bosons can be identified with the would-be Goldstones. For instance,

$$T(W_L^a W_L^b \to W_L^c W_L^d) = T(\omega^a \omega^b \to \omega^c \omega^d) + \mathcal{O}\left(M_W/\sqrt{s}\right)$$

- The EWSBS behaves as if the would-be Goldstone bosons were physical states. The non-gauged Lagragian can be used directly to compute scattering amplitudes.
- During the 90's, the limits of applicability of this theorem were studied in detail, leading to the conclusion that it is valid for chiral Lagrangians, like those used in this presentation:

  works from W.B.Kilgore, P.B.Pal, X.Zhang, A.Dobado, J.R.Peláez, M.T.Urdiales, H.-J.He, Y.-P.Kuang, D.Espriu, J.Matias, J.F.Donoghue, J.Tandean,...

Equivalence Theorem

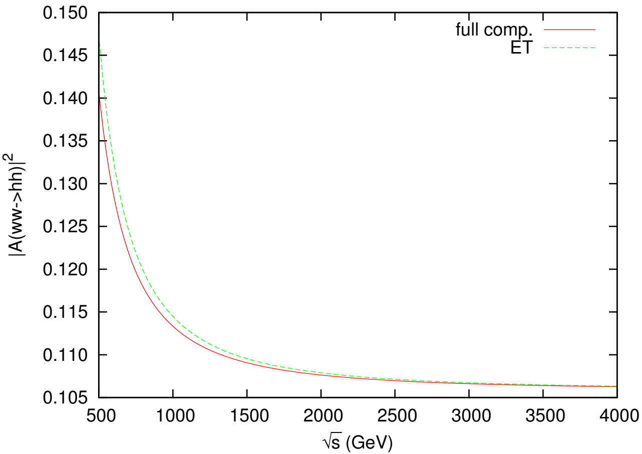

Comparison between the full LO $\omega\omega \to hh$ ($\cos\theta = 3$) and that computed through the ET. The SM is used here. Work in collaboration with S. Moretti, to test a modified version of MadGraph.

Non-linear Electroweak Chiral Lagrangian

We have no clue of what, how or if new physics...
Non-linear EFT[2] for VV scattering at NLO level, minimally coupled to hh,

$$\mathcal{L} = \frac{v^2}{4} g(h/f)\,\mathrm{Tr}[(D_\mu U)^\dagger D^\mu U] + \frac{1}{2}\partial_\mu h \partial^\mu h - V(h),$$

where

$$g(h/v) = 1 + 2a\frac{h}{v} + b\left(\frac{h}{v}\right)^2 + \ldots$$

$$V(h) = V_0 + \frac{M_h^2}{2}h^2 + \sum_{n=3}^{\infty}\lambda_n h^n$$

$$D_\mu U = \partial_\mu U + i\hat{W}_\mu U - iU\hat{B}_\mu.$$

M_h and λ_n are subleading in chiral counting.

[2] Yellow Report: *C.Grojean, A.Falkowski, M.Trott, B.Fuks, *G.Buchalla, T.Plehn, G.Isidori, K.Tackmann, L.Brenner,...; CERN-2017-002-M.

Non-linear Electroweak Chiral Lagrangian

We have no clue of what, how or if new physics...
Non-linear EFT[2] for VV scattering at NLO level, minimally coupled to hh,

$$\mathcal{L} = \frac{v^2}{4} g(h/f)\, \mathrm{Tr}[(D_\mu U)^\dagger D^\mu U] + \frac{1}{2}\partial_\mu h \partial^\mu h - V(h),$$

where

$$g(h/v) = 1 + 2a\frac{h}{v} + b\left(\frac{h}{v}\right)^2 + \dots$$

$$V(h) = V_0 + \frac{M_h^2}{2} h^2 + \sum_{n=3}^{\infty} \lambda_n h^n$$

$$D_\mu U = \partial_\mu U + i\hat{W}_\mu U - iU\hat{B}_\mu.$$

M_h and λ_n are subleading in chiral counting.

[2] Yellow Report: *C.Grojean, A.Falkowski, M.Trott, B.Fuks, *G.Buchalla, T.Plehn, G.Isidori, K.Tackmann, L.Brenner,...; CERN-2017-002-M.

Non-linear Electroweak Chiral Lagrangian

We have no clue of what, how or if new physics...
Non-linear EFT[2] for VV scattering at NLO level, minimally coupled to hh,

$$\mathcal{L} = \frac{v^2}{4} g(h/f)\, \mathrm{Tr}[(D_\mu U)^\dagger D^\mu U] + \frac{1}{2}\partial_\mu h \partial^\mu h - V(h),$$

where

$$g(h/v) = 1 + 2a\frac{h}{v} + b\left(\frac{h}{v}\right)^2 + \ldots$$

$$V(h) = V_0 + \frac{M_h^2}{2} h^2 + \sum_{n=3}^{\infty} \lambda_n h^n$$

$$D_\mu U = \partial_\mu U + i\hat{W}_\mu U - iU\hat{B}_\mu .$$

M_h and λ_n are subleading in chiral counting.

[2] Yellow Report: *C.Grojean, A.Falkowski, M.Trott, B.Fuks, *G.Buchalla, T.Plehn, G.Isidori, K.Tackmann, L.Brenner,...; CERN-2017-002-M.

Non-linear Electroweak Chiral Lagrangian

We need the parameterization of the $U(\omega^a) \in SU(2)_L \times SU(2)_R / SU(2)_C$ coset. In either case, whatever the non–linear term is,

$$U(x) = \mathbb{1} + i\frac{\tau^a \omega^a(x)}{v} + \mathcal{O}\left(\omega^2\right).$$

Two choices have been used:

Spherical parameterization

$$U(x) = \mathbb{1}\sqrt{1 - \frac{\omega^2(x)}{v^2}} + i\frac{\tau^a \omega^a(x)}{v}$$

Exponential parameterization (here, a cross-check for EWSBS+$\gamma\gamma$)

$$U(x) = \exp\left(i\frac{\tau^a \pi^a(x)}{v}\right)$$

Non-linear Electroweak Chiral Lagrangian

We need the parameterization of the $U(\omega^a) \in SU(2)_L \times SU(2)_R / SU(2)_C$ coset. In either case, whatever the non–linear term is,

$$U(x) = \mathbb{1} + i\frac{\tau^a \omega^a(x)}{v} + \mathcal{O}\left(\omega^2\right).$$

Two choices have been used:

Spherical parameterization

$$U(x) = \mathbb{1}\sqrt{1 - \frac{\omega^2(x)}{v^2}} + i\frac{\tau^a \omega^a(x)}{v}$$

Exponential parameterization (here, a cross-check for EWSBS+$\gamma\gamma$)

$$U(x) = \exp\left(i\frac{\tau^a \pi^a(x)}{v}\right)$$

Non-linear Electroweak Chiral Lagrangian

We need the parameterization of the $U(\omega^a) \in SU(2)_L \times SU(2)_R / SU(2)_C$ coset. In either case, whatever the non–linear term is,

$$U(x) = \mathbb{1} + i\frac{\tau^a \omega^a(x)}{v} + \mathcal{O}\left(\omega^2\right) .$$

Two choices have been used:

Spherical parameterization

$$U(x) = \mathbb{1}\sqrt{1 - \frac{\omega^2(x)}{v^2}} + i\frac{\tau^a \omega^a(x)}{v}$$

Exponential parameterization (here, a cross-check for EWSBS+$\gamma\gamma$)

$$U(x) = \exp\left(i\frac{\tau^a \pi^a(x)}{v}\right)$$

Non-linear Electroweak Chiral Lagrangian

We need the parameterization of the $U(\omega^a) \in SU(2)_L \times SU(2)_R / SU(2)_C$ coset. In either case, whatever the non–linear term is,

$$U(x) = \mathbb{1} + i\frac{\tau^a \omega^a(x)}{v} + \mathcal{O}\left(\omega^2\right) .$$

Two choices have been used:

Spherical parameterization

$$U(x) = \mathbb{1}\sqrt{1 - \frac{\omega^2(x)}{v^2}} + i\frac{\tau^a \omega^a(x)}{v}$$

Exponential parameterization (here, a cross-check for EWSBS+$\gamma\gamma$)

$$U(x) = \exp\left(i\frac{\tau^a \pi^a(x)}{v}\right)$$

EFT for VV scattering, minimally coupled to hh

Since we are considering scattering processes within the EWSBS, the covariant derivate reduces to

$$D_\mu U = \partial_\mu U.$$

Define

$$V_\mu \equiv (D_\mu U)U^\dagger.$$

The next counterterms are needed for the NLO computation of the VV scattering, minimally coupled to hh

$$\begin{aligned}\mathcal{L}_4 = {} & a_4[\mathrm{Tr}(V_\mu V_\nu)][\mathrm{Tr}(V^\mu V^\nu)] + a_5[\mathrm{Tr}(V_\mu V^\mu)][\mathrm{Tr}(V_\nu V^\nu)] \\ & + \frac{d}{v^2}(\partial_\mu h \partial^\mu h)\,\mathrm{Tr}[(D_\nu U)^\dagger D^\nu U] + \frac{e}{v^2}(\partial_\mu h \partial^\nu h)\,\mathrm{Tr}[(D^\mu U)^\dagger D_\nu U] \\ & + \frac{g}{v^4}(\partial_\mu h \partial^\mu h)(\partial_\nu h \partial^\nu h).\end{aligned}$$

EFT for VV scattering, minimally coupled to hh

Since we are considering scattering processes within the EWSBS, the covariant derivate reduces to

$$D_\mu U = \partial_\mu U.$$

Define

$$V_\mu \equiv (D_\mu U)U^\dagger.$$

The next counterterms are needed for the NLO computation of the VV scattering, minimally coupled to hh

$$\mathcal{L}_4 = a_4[\mathrm{Tr}(V_\mu V_\nu)][\mathrm{Tr}(V^\mu V^\nu)] + a_5[\mathrm{Tr}(V_\mu V^\mu)][\mathrm{Tr}(V_\nu V^\nu)] \\ + \frac{d}{v^2}(\partial_\mu h \partial^\mu h)\,\mathrm{Tr}[(D_\nu U)^\dagger D^\nu U] + \frac{e}{v^2}(\partial_\mu h \partial^\nu h)\,\mathrm{Tr}[(D^\mu U)^\dagger D_\nu U] \\ + \frac{g}{v^4}(\partial_\mu h \partial^\mu h)(\partial_\nu h \partial^\nu h).$$

EFT for VV scattering, minimally coupled to hh

Since we are considering scattering processes within the EWSBS, the covariant derivate reduces to

$$D_\mu U = \partial_\mu U.$$

Define

$$V_\mu \equiv (D_\mu U)U^\dagger.$$

The next counterterms are needed for the NLO computation of the VV scattering, minimally coupled to hh

$$\begin{aligned}\mathcal{L}_4 = {} & a_4[\mathrm{Tr}(V_\mu V_\nu)][\mathrm{Tr}(V^\mu V^\nu)] + a_5[\mathrm{Tr}(V_\mu V^\mu)][\mathrm{Tr}(V_\nu V^\nu)] \\ & + \frac{d}{v^2}(\partial_\mu h \partial^\mu h)\,\mathrm{Tr}[(D_\nu U)^\dagger D^\nu U] + \frac{e}{v^2}(\partial_\mu h \partial^\nu h)\,\mathrm{Tr}[(D^\mu U)^\dagger D_\nu U] \\ & + \frac{g}{v^4}(\partial_\mu h \partial^\mu h)(\partial_\nu h \partial^\nu h).\end{aligned}$$

EFT for VV scattering, minimally coupled to hh

Since we are considering scattering processes within the EWSBS, the covariant derivate reduces to

$$D_\mu U = \partial_\mu U.$$

Define

$$V_\mu \equiv (D_\mu U)U^\dagger.$$

The next counterterms are needed for the NLO computation of the VV scattering, minimally coupled to hh

$$\mathcal{L}_4 = a_4[\mathrm{Tr}(V_\mu V_\nu)][\mathrm{Tr}(V^\mu V^\nu)] + a_5[\mathrm{Tr}(V_\mu V^\mu)][\mathrm{Tr}(V_\nu V^\nu)]$$
$$+ \frac{d}{v^2}(\partial_\mu h \partial^\mu h)\,\mathrm{Tr}[(D_\nu U)^\dagger D^\nu U] + \frac{e}{v^2}(\partial_\mu h \partial^\nu h)\,\mathrm{Tr}[(D^\mu U)^\dagger D_\nu U]$$
$$+ \frac{g}{v^4}(\partial_\mu h \partial^\mu h)(\partial_\nu h \partial^\nu h).$$

EFT for VV scattering, minimally coupled to hh

Since we are considering scattering processes within the EWSBS, the covariant derivate reduces to

$$D_\mu U = \partial_\mu U.$$

Define

$$V_\mu \equiv (D_\mu U)U^\dagger.$$

The next counterterms are needed for the NLO computation of the VV scattering, minimally coupled to hh

$$\mathcal{L}_4 = a_4[\mathrm{Tr}(V_\mu V_\nu)][\mathrm{Tr}(V^\mu V^\nu)] + a_5[\mathrm{Tr}(V_\mu V^\mu)][\mathrm{Tr}(V_\nu V^\nu)] + \frac{d}{v^2}(\partial_\mu h \partial^\mu h)\,\mathrm{Tr}[(D_\nu U)^\dagger D^\nu U] + \frac{e}{v^2}(\partial_\mu h \partial^\nu h)\,\mathrm{Tr}[(D^\mu U)^\dagger D_\nu U] + \frac{g}{v^4}(\partial_\mu h \partial^\mu h)(\partial_\nu h \partial^\nu h).$$

EFT for VV scattering, minimally coupled to hh

Since we are considering scattering processes within the EWSBS, the covariant derivate reduces to

$$D_\mu U = \partial_\mu U.$$

Define

$$V_\mu \equiv (D_\mu U) U^\dagger.$$

The next counterterms are needed for the NLO computation of the VV scattering, minimally coupled to hh

$$\begin{aligned}\mathcal{L}_4 = a_4 [\mathrm{Tr}(V_\mu V_\nu)][\mathrm{Tr}(V^\mu V^\nu)] + a_5 [\mathrm{Tr}(V_\mu V^\mu)][\mathrm{Tr}(V_\nu V^\nu)] \\ + \frac{d}{v^2}(\partial_\mu h \partial^\mu h)\,\mathrm{Tr}[(D_\nu U)^\dagger D^\nu U] + \frac{e}{v^2}(\partial_\mu h \partial^\nu h)\,\mathrm{Tr}[(D^\mu U)^\dagger D_\nu U] \\ + \frac{g}{v^4}(\partial_\mu h \partial^\mu h)(\partial_\nu h \partial^\nu h).\end{aligned}$$

EFT for VV scattering, minimally coupled to hh

Using the spherical parameterization for the $SU(2)$ coset and neglecting the couplings with photons and quarks, we have the next Lagrangian describing $VV \to VV$, $VV \to hh$ and $hh \to hh$ processes:

$$\begin{aligned}
\mathcal{L} &= \left[1 + 2a\frac{h}{v} + b\left(\frac{h}{v}\right)^2\right]\frac{\partial_\mu\omega^a\partial^\mu\omega^b}{2}\left(\delta^{ab} + \frac{\omega^a\omega^b}{v^2}\right) \\
&+ \frac{4a_4}{v^4}\partial_\mu\omega^a\partial_\nu\omega^a\partial^\mu\omega^b\partial^\nu\omega^b + \frac{4a_5}{v^4}\partial_\mu\omega^a\partial^\mu\omega^a\partial_\nu\omega^b\partial^\nu\omega^b \\
&+ \frac{2d}{v^4}\partial_\mu h\partial^\mu h\partial_\nu\omega^a\partial^\nu\omega^a + \frac{2e}{v^4}\partial_\mu h\partial^\mu\omega^a\partial_\nu h\partial^\nu\omega^a \\
&+ \frac{1}{2}\partial_\mu h\partial^\mu h + \frac{g}{v^4}(\partial_\mu h\partial^\mu h)^2
\end{aligned}$$

Extension to $\gamma\gamma$ states

Since coupling with photons are considered[3], the covariant derivative is defined as

$$D_\mu U = \partial_\mu U + i\hat{W}_\mu U - iU\hat{B}_\mu .$$

The photon field A arises from the couplings with $\hat{W}_{\mu\nu}$ and $\hat{B}_{\mu\nu}$ through a rotation to the physical basis; an anomalous three-particle coupling may appear

$$-c_W \frac{h}{v} \hat{W}_{\mu\nu}\hat{W}^{\mu\nu} - c_B \frac{h}{v}\hat{B}_{\mu\nu}\hat{B}^{\mu\nu} = -\frac{c_\gamma}{2}\frac{h}{v} e^2 A_{\mu\nu}A^{\mu\nu}$$

The next additional NLO counterterms are needed,

$$\begin{aligned}\mathcal{L}_{4'} = a_1 \operatorname{Tr}(U\hat{B}_{\mu\nu}U^\dagger \hat{W}^{\mu\nu}) \\ + ia_2 \operatorname{Tr}(U\hat{B}_{\mu\nu}U^\dagger [V^\mu, V^\nu]) \\ - ia_3 \operatorname{Tr}(\hat{W}_{\mu\nu}[V^\mu, V^\nu])\end{aligned}$$

[3]Work in collaboration with M.J.Herrero and J.J.Sanz-Cillero, JHEP**1407** (2014) 149.

Extension to $\gamma\gamma$ states

Since coupling with photons are considered[3], the covariant derivative is defined as

$$D_\mu U = \partial_\mu U + i\hat{W}_\mu U - iU\hat{B}_\mu .$$

The photon field A arises from the couplings with $\hat{W}_{\mu\nu}$ and $\hat{B}_{\mu\nu}$ through a rotation to the physical basis; an anomalous three-particle coupling may appear

$$-c_W \frac{h}{v} \hat{W}_{\mu\nu} \hat{W}^{\mu\nu} - c_B \frac{h}{v} \hat{B}_{\mu\nu} \hat{B}^{\mu\nu} = -\frac{c_\gamma}{2} \frac{h}{v} e^2 A_{\mu\nu} A^{\mu\nu}$$

The next additional NLO counterterms are needed,

$$\begin{aligned}\mathcal{L}_{4'} = {} & a_1 \operatorname{Tr}(U\hat{B}_{\mu\nu}U^\dagger \hat{W}^{\mu\nu}) \\ & + ia_2 \operatorname{Tr}(U\hat{B}_{\mu\nu}U^\dagger [V^\mu, V^\nu]) \\ & - ia_3 \operatorname{Tr}(\hat{W}_{\mu\nu}[V^\mu, V^\nu])\end{aligned}$$

[3]Work in collaboration with M.J.Herrero and J.J.Sanz-Cillero, JHEP **1407** (2014) 149.

Extension to $\gamma\gamma$ states

Since coupling with photons are considered[3], the covariant derivative is defined as

$$D_\mu U = \partial_\mu U + i\hat{W}_\mu U - iU\hat{B}_\mu .$$

The photon field A arises from the couplings with $\hat{W}_{\mu\nu}$ and $\hat{B}_{\mu\nu}$ through a rotation to the physical basis; an anomalous three-particle coupling may appear

$$-c_W \frac{h}{v}\hat{W}_{\mu\nu}\hat{W}^{\mu\nu} - c_B \frac{h}{v}\hat{B}_{\mu\nu}\hat{B}^{\mu\nu} = -\frac{c_\gamma}{2}\frac{h}{v}e^2 A_{\mu\nu}A^{\mu\nu}$$

The next additional NLO counterterms are needed,

$$\begin{aligned}\mathcal{L}_{4'} = {} & a_1 \operatorname{Tr}(U\hat{B}_{\mu\nu}U^\dagger \hat{W}^{\mu\nu}) \\ & + ia_2 \operatorname{Tr}(U\hat{B}_{\mu\nu}U^\dagger [V^\mu, V^\nu]) \\ & - ia_3 \operatorname{Tr}(\hat{W}_{\mu\nu}[V^\mu, V^\nu])\end{aligned}$$

[3]Work in collaboration with M.J.Herrero and J.J.Sanz-Cillero, JHEP**1407** (2014) 149.

Extension to $\gamma\gamma$ states

Since coupling with photons are considered[3], the covariant derivative is defined as

$$D_\mu U = \partial_\mu U + i\hat{W}_\mu U - iU\hat{B}_\mu.$$

The photon field A arises from the couplings with $\hat{W}_{\mu\nu}$ and $\hat{B}_{\mu\nu}$ through a rotation to the physical basis; an anomalous three-particle coupling may appear

$$-c_W \frac{h}{v}\hat{W}_{\mu\nu}\hat{W}^{\mu\nu} - c_B \frac{h}{v}\hat{B}_{\mu\nu}\hat{B}^{\mu\nu} = -\frac{c_\gamma}{2}\frac{h}{v}e^2 A_{\mu\nu}A^{\mu\nu}$$

The next additional NLO counterterms are needed,

$$\mathcal{L}_{4'} = a_1 \operatorname{Tr}(U\hat{B}_{\mu\nu}U^\dagger \hat{W}^{\mu\nu})$$
$$+ ia_2 \operatorname{Tr}(U\hat{B}_{\mu\nu}U^\dagger[V^\mu, V^\nu])$$
$$- ia_3 \operatorname{Tr}(\hat{W}_{\mu\nu}[V^\mu, V^\nu])$$

[3]Work in collaboration with M.J.Herrero and J.J.Sanz-Cillero, JHEP**1407** (2014) 149.

Extension to $\gamma\gamma$ states

Since coupling with photons are considered[3], the covariant derivative is defined as

$$D_\mu U = \partial_\mu U + i\hat{W}_\mu U - iU\hat{B}_\mu .$$

The photon field A arises from the couplings with $\hat{W}_{\mu\nu}$ and $\hat{B}_{\mu\nu}$ through a rotation to the physical basis; an anomalous three-particle coupling may appear

$$-c_W \frac{h}{v}\hat{W}_{\mu\nu}\hat{W}^{\mu\nu} - c_B \frac{h}{v}\hat{B}_{\mu\nu}\hat{B}^{\mu\nu} = -\frac{c_\gamma}{2}\frac{h}{v}e^2 A_{\mu\nu}A^{\mu\nu}$$

The next additional NLO counterterms are needed,

$$\begin{aligned}\mathcal{L}_{4'} = {}& a_1 \operatorname{Tr}(U\hat{B}_{\mu\nu}U^\dagger \hat{W}^{\mu\nu}) \\ & + ia_2 \operatorname{Tr}(U\hat{B}_{\mu\nu}U^\dagger [V^\mu, V^\nu]) \\ & - ia_3 \operatorname{Tr}(\hat{W}_{\mu\nu}[V^\mu, V^\nu])\end{aligned}$$

[3]Work in collaboration with M.J.Herrero and J.J.Sanz-Cillero, JHEP**1407** (2014) 149.

Extension to $\gamma\gamma$ states

Since coupling with photons are considered[3], the covariant derivative is defined as

$$D_\mu U = \partial_\mu U + i\hat{W}_\mu U - iU\hat{B}_\mu .$$

The photon field A arises from the couplings with $\hat{W}_{\mu\nu}$ and $\hat{B}_{\mu\nu}$ through a rotation to the physical basis; an anomalous three-particle coupling may appear

$$-c_W \frac{h}{v}\hat{W}_{\mu\nu}\hat{W}^{\mu\nu} - c_B \frac{h}{v}\hat{B}_{\mu\nu}\hat{B}^{\mu\nu} = -\frac{c_\gamma}{2}\frac{h}{v}e^2 A_{\mu\nu}A^{\mu\nu}$$

The next additional NLO counterterms are needed,

$$\begin{aligned}\mathcal{L}_{4'} = {} & a_1 \,\mathrm{Tr}(U\hat{B}_{\mu\nu}U^\dagger \hat{W}^{\mu\nu}) \\ & + ia_2 \,\mathrm{Tr}(U\hat{B}_{\mu\nu}U^\dagger [V^\mu, V^\nu]) \\ & - ia_3 \,\mathrm{Tr}(\hat{W}_{\mu\nu}[V^\mu, V^\nu])\end{aligned}$$

[3]Work in collaboration with M.J.Herrero and J.J.Sanz-Cillero, JHEP**1407** (2014) 149.

Extension to $t\bar{t}$ states

Lagrangian additions[4]:

$$\mathcal{L}' = i\bar{Q}\partial Q - v\mathcal{G}(h)\left[\bar{Q}'_L U H_Q Q'_R + h.c.\right].$$

This expression, for the heaviest quark generation, expands to[5]

$$\mathcal{L}_Y = -\mathcal{G}(h)\left\{\sqrt{1-\frac{\omega^2}{v^2}}\left(M_t t\bar{t} + M_b\bar{b}b\right) + \frac{i\omega^0}{v}\left(M_t\bar{t}\gamma^5 t - M_b\bar{b}\gamma^5 b\right)\right.$$
$$\left. + \frac{i\sqrt{2}\omega^+}{v}\left(M_b\bar{t}_L b_R - M_t\bar{t}_R b_L\right) + \frac{i\sqrt{2}\omega^-}{v}\left(M_t\bar{b}_L t_R - M_b\bar{b}_R t_L\right)\right\}$$

Two NLO counterterms needed for renormalization,

$$\mathcal{L}_{4''} = g_t\frac{M_t}{v^4}\partial_\mu\omega^a\partial^\mu\omega^b t\bar{t} + g'_t\frac{M_t}{v^4}\partial_\mu h\partial^\mu h t\bar{t}$$

[4] Work in collaboration with A.Castillo, arXiv:1607.01158 [hep-ph], accepted in EPJC.

[5] $\mathcal{G}(h) = 1 + c_1(h/v) + c_2(h/v)^2 + \dots$, V_{tb} very close to unity

Extension to $t\bar{t}$ states

Lagrangian additions[4]:

$$\mathcal{L}' = i\bar{Q}\partial Q - v\mathcal{G}(h)\left[\bar{Q}'_L U H_Q Q'_R + h.c.\right].$$

This expression, for the heaviest quark generation, expands to[5]

$$\mathcal{L}_Y = -\mathcal{G}(h)\left\{\sqrt{1-\frac{\omega^2}{v^2}}\left(M_t t\bar{t} + M_b \bar{b}b\right) + \frac{i\omega^0}{v}\left(M_t \bar{t}\gamma^5 t - M_b \bar{b}\gamma^5 b\right) + \frac{i\sqrt{2}\omega^+}{v}\left(M_b \bar{t}_L b_R - M_t \bar{t}_R b_L\right) + \frac{i\sqrt{2}\omega^-}{v}\left(M_t \bar{b}_L t_R - M_b \bar{b}_R t_L\right)\right\}$$

Two NLO counterterms needed for renormalization,

$$\mathcal{L}_{4''} = g_t \frac{M_t}{v^4}\partial_\mu \omega^a \partial^\mu \omega^b t\bar{t} + g'_t \frac{M_t}{v^4}\partial_\mu h \partial^\mu h t\bar{t}$$

[4]Work in collaboration with A.Castillo, arXiv:1607.01158 [hep-ph], accepted in EPJC.
[5]$\mathcal{G}(h) = 1 + c_1(h/v) + c_2(h/v)^2 + \ldots$, V_{tb} very close to unity

Extension to $t\bar{t}$ states

Lagrangian additions[4]:

$$\mathcal{L}' = i\bar{Q}\partial Q - v\mathcal{G}(h)\left[\bar{Q}'_L U H_Q Q'_R + h.c.\right].$$

This expression, for the heaviest quark generation, expands to[5]

$$\mathcal{L}_Y = -\mathcal{G}(h)\Bigg\{\sqrt{1-\frac{\omega^2}{v^2}}\left(M_t t\bar{t} + M_b\bar{b}b\right) + \frac{i\omega^0}{v}\left(M_t\bar{t}\gamma^5 t - M_b\bar{b}\gamma^5 b\right)$$
$$+\frac{i\sqrt{2}\omega^+}{v}\left(M_b\bar{t}_L b_R - M_t\bar{t}_R b_L\right) + \frac{i\sqrt{2}\omega^-}{v}\left(M_t\bar{b}_L t_R - M_b\bar{b}_R t_L\right)\Bigg\}$$

Two NLO counterterms needed for renormalization,

$$\mathcal{L}_{4''} = g_t\frac{M_t}{v^4}\partial_\mu\omega^a\partial^\mu\omega^b t\bar{t} + g'_t\frac{M_t}{v^4}\partial_\mu h\partial^\mu h t\bar{t}$$

[4] Work in collaboration with A.Castillo, arXiv:1607.01158 [hep-ph], accepted in EPJC.
[5] $\mathcal{G}(h) = 1 + c_1(h/v) + c_2(h/v)^2 + \ldots$, V_{tb} very close to unity

Chiral counting

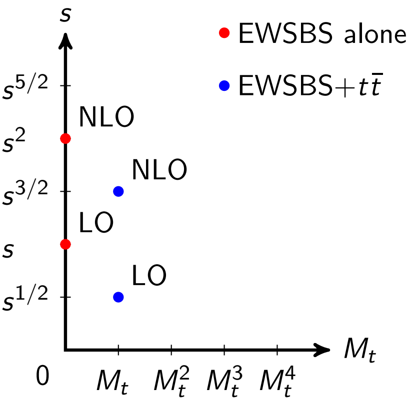

Note the usage of the chiral counting from[6].

[6] G.Buchalla and O.Catà, JHEP**07** (2012) 101; G.Buchalla, O.Catà and C.Krause, Phys.Lett.**B731** (2014) 80; S.Weinberg, Physica **A96** (1979) 327.

Chiral counting

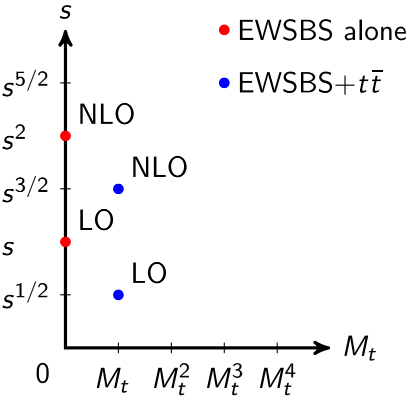

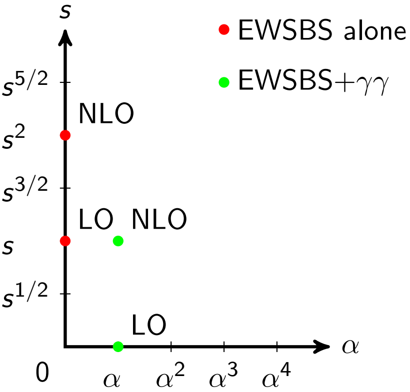

Note the usage of the chiral counting from[6].

[6] G.Buchalla and O.Catà, JHEP**07** (2012) 101; G.Buchalla, O.Catà and C.Krause, Phys.Lett.**B731** (2014) 80; S.Weinberg, Physica **A96** (1979) 327

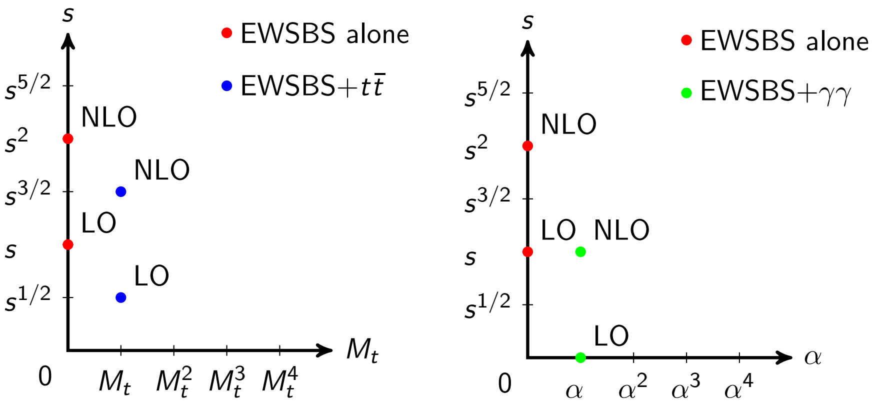

Note the usage of the chiral counting from[6].

[6] G.Buchalla and O.Catà, JHEP**07** (2012) 101; G.Buchalla, O.Catà and C.Krause, Phys.Lett.**B731** (2014) 80; S.Weinberg, Physica **A96** (1979) 327.

Particular cases of the theory

$a^2 = b = 0$

Higgsless ECL, now experimentally discarded.
J.Gasser and H.Leutwyler, Annal.Phys.**158**,142; Nucl.Phys.B**250**,465&517

$a^2 = 1 - v^2/f^2$, $b = 1 - 2v^2/f^2$

$SO(5)/SO(4)$ Minimal Composite Higgs Model (MCHM)
K.Agashe, R.Contino and A.Pomarol, Nucl.Phys.B**719**, 165
S.De Curtis, S.Moretti, K.Yagyu, E.Yildirim, JHEP**1204** (2012) 042

$a^2 = b = v^2/f^2$

Dilaton models
E.Halyo, Mod.Phys.Lett.A**8**, 275; W.D.Goldberg et al, PRL**100** 111802

$a^2 = b = 1$

Standard Model: without non-perturbative interactions

Particular cases of the theory

$a^2 = b = 0$

Higgsless ECL, now experimentally discarded.
J.Gasser and H.Leutwyler, Annal.Phys.**158**,142; Nucl.Phys.B**250**,465&517

$a^2 = 1 - v^2/f^2$, $b = 1 - 2v^2/f^2$

$SO(5)/SO(4)$ Minimal Composite Higgs Model (MCHM)
K.Agashe, R.Contino and A.Pomarol, Nucl.Phys.B**719**, 165
S.De Curtis, S.Moretti, K.Yagyu, E.Yildirim, JHEP**1204** (2012) 042

$a^2 = b = v^2/f^2$

Dilaton models
E.Halyo, Mod.Phys.Lett.A**8**, 275; W.D.Goldberg et al, PRL**100** 111802

$a^2 = b = 1$

Standard Model: without non-perturbative interactions

Particular cases of the theory

$a^2 = b = 0$

Higgsless ECL, now experimentally discarded.
J.Gasser and H.Leutwyler, Annal.Phys.**158**,142; Nucl.Phys.B**250**,465&517

$a^2 = 1 - v^2/f^2$, $b = 1 - 2v^2/f^2$

$SO(5)/SO(4)$ Minimal Composite Higgs Model (MCHM)
K.Agashe, R.Contino and A.Pomarol, Nucl.Phys.B**719**, 165
S.De Curtis, S.Moretti, K.Yagyu, E.Yildirim, JHEP**1204** (2012) 042

$a^2 = b = v^2/f^2$

Dilaton models
E.Halyo, Mod.Phys.Lett.A**8**, 275; W.D.Goldberg et al, PRL**100** 111802

$a^2 = b = 1$

Standard Model: without non-perturbative interactions

Particular cases of the theory

$a^2 = b = 0$

Higgsless ECL, now experimentally discarded.
J.Gasser and H.Leutwyler, Annal.Phys.**158**,142; Nucl.Phys.B**250**,465&517

$a^2 = 1 - v^2/f^2$, $b = 1 - 2v^2/f^2$

$SO(5)/SO(4)$ Minimal Composite Higgs Model (MCHM)
K.Agashe, R.Contino and A.Pomarol, Nucl.Phys.B**719**, 165
S.De Curtis, S.Moretti, K.Yagyu, E.Yildirim, JHEP**1204** (2012) 042

$a^2 = b = v^2/f^2$

Dilaton models
E.Halyo, Mod.Phys.Lett.A**8**, 275; W.D.Goldberg et al, PRL**100** 111802

$a^2 = b = 1$

Standard Model: without non-perturbative interactions

Experimental bounds on low-energy constants

- As it would require measuring the coupling of two Higgses, there is no experimental bound over the value of b parameter[7] . Over a, at a confidence level of 2σ (95%),
  - CMS[8] .... $a \in (0.87, 1.14)$
  - ATLAS[9] .... $a \in (0.93, 1.34)$
  - Fit of Buchalla et. al.[10] .... $a \in (0.80, 1.16)$

[7] Giardino, P.P., *Aspects of LHC phenom.*, PhD Thesis (2013), Università di Pisa

[8] Eur. Phys. J. **C75** (2015), 212

[9] Report No. ATLAS-CONF-2014-009

[10] G. Buchalla, O. Cata, A. Celis, and C. Krause, Eur.Phys.J. C76 (2016) no.5, 233

Experimental bounds on low-energy constants

- As it would require measuring the coupling of two Higgses, there is no experimental bound over the value of b parameter[7] . Over a, at a confidence level of 2σ (95%),
  - CMS[8] . . . . $a \in (0.87, 1.14)$
  - ATLAS[9] . . . . $a \in (0.93, 1.34)$
  - Fit of Buchalla et. al.[10] . . . . $a \in (0.80, 1.16)$

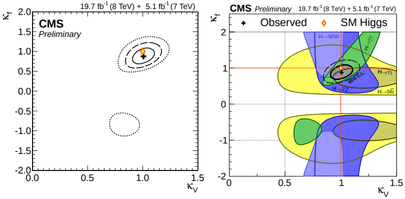

[7]Giardino, P.P., *Aspects of LHC phenom.*, PhD Thesis (2013), Università di Pisa
[8]Eur. Phys. J. **C75** (2015), 212
[9]Report No. ATLAS-CONF-2014-009
[10]G. Buchalla, O. Cata, A. Celis, and C. Krause, Eur.Phys.J. C76 (2016) no.5, 233

Experimental bounds on low-energy constants

- As it would require measuring the coupling of two Higgses, there is no experimental bound over the value of b parameter[7] . Over a, at a confidence level of 2σ (95%),
  - CMS[8] .... $a \in (0.87, 1.14)$
  - ATLAS[9] .... $a \in (0.93, 1.34)$
  - Fit of Buchalla et. al.[10] .... $a \in (0.80, 1.16)$

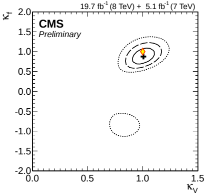

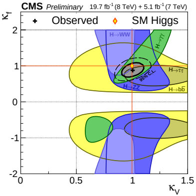

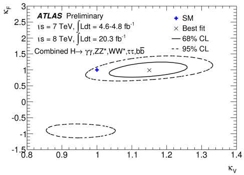

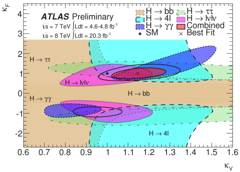

[7] Giardino, P.P., *Aspects of LHC phenom.*, PhD Thesis (2013), Università di Pisa
[8] Eur. Phys. J. **C75** (2015), 212
[9] Report No. ATLAS-CONF-2014-009
[10] G. Buchalla, O. Cata, A. Celis, and C. Krause, Eur.Phys.J. C76 (2016) no.5, 233

Experimental bounds on low-energy constants

- As it would require measuring the coupling of two Higgses, there is no experimental bound over the value of b parameter[7] . Over a, at a confidence level of 2σ (95%),
  - CMS[8] .... $a \in (0.87, 1.14)$
  - ATLAS[9] .... $a \in (0.93, 1.34)$
  - Fit of Buchalla et. al.[10] .... $a \in (0.80, 1.16)$

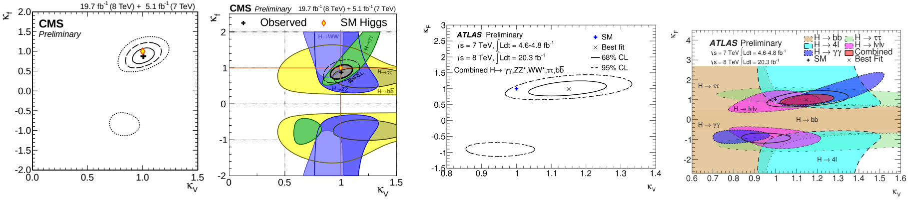

[7]Giardino, P.P., *Aspects of LHC phenom.*, PhD Thesis (2013), Università di Pisa
[8]Eur. Phys. J. **C75** (2015), 212
[9]Report No. ATLAS-CONF-2014-009
[10]G. Buchalla, O. Cata, A. Celis, and C. Krause, Eur.Phys.J. C**76** (2016) no.5, 233

Experimental bounds on low-energy constants, NLO a_4-a_5

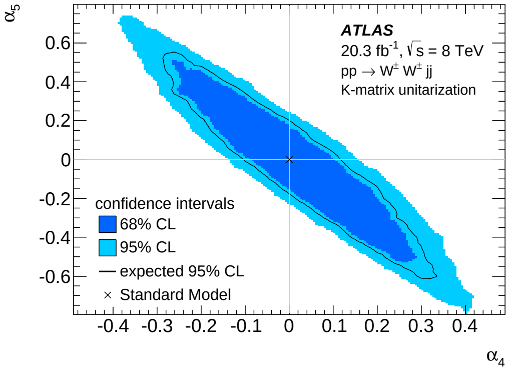

Direct constraint over a_4-a_5 from ATLAS Collaboration[11]

[11] Taken from ref. [PRL**113** (2014) 141803]. Note that CMS [PRL**114** (2015) 051801] gives a constraint in terms of F_{S0}/Λ^4 and F_{S1}/Λ^4 parameters, which have no direct translation to the a_4 and a_5 ones [arXiv:1310.6708, [hep-ph]].

Partial wave decomposition

EWSBS alone (+eventually $t\bar{t}$)

$$A_{IJ}(s) = \frac{1}{32\pi K}\int_{-1}^{1} dx\, P_J(x) A_I[s, t(s,x), u(s,x)]$$

Matrix element from partial wave decomposition

$$A_I(s,t,u) = 16\pi K \sum_{J=0}^{\infty}(2J+1)P_J[x(s,t)]A_{IJ}(s)$$

Helicity partial waves for EWSBS+$\gamma\gamma$

$$F_{IJ}^{\lambda_1\lambda_2}(s) = \frac{1}{64\pi^2 K}\sqrt{\frac{4\pi}{2J+1}}\int d\Omega\, A_I^{\lambda_1\lambda_2}(s,\Omega)\, Y_{J,\lambda_1-\lambda_2}(\Omega)$$

Partial wave decomposition

EWSBS alone (+eventually $t\bar{t}$)

$$A_{IJ}(s) = \frac{1}{32\pi K}\int_{-1}^{1} dx\, P_J(x) A_I[s, t(s,x), u(s,x)]$$

Matrix element from partial wave decomposition

$$A_I(s,t,u) = 16\pi K \sum_{J=0}^{\infty}(2J+1)P_J[x(s,t)]A_{IJ}(s)$$

Helicity partial waves for EWSBS+$\gamma\gamma$

$$F_{IJ}^{\lambda_1\lambda_2}(s) = \frac{1}{64\pi^2 K}\sqrt{\frac{4\pi}{2J+1}}\int d\Omega\, A_I^{\lambda_1\lambda_2}(s,\Omega) Y_{J,\lambda_1-\lambda_2}(\Omega)$$

Partial wave decomposition

EWSBS alone (+eventually $t\bar{t}$)

$$A_{IJ}(s) = \frac{1}{32\pi K}\int_{-1}^{1} dx\, P_J(x) A_I[s, t(s,x), u(s,x)]$$

Matrix element from partial wave decomposition

$$A_I(s,t,u) = 16\pi K \sum_{J=0}^{\infty} (2J+1) P_J[x(s,t)] A_{IJ}(s)$$

Helicity partial waves for EWSBS+$\gamma\gamma$

$$F_{IJ}^{\lambda_1\lambda_2}(s) = \frac{1}{64\pi^2 K}\sqrt{\frac{4\pi}{2J+1}}\int d\Omega\, A_I^{\lambda_1\lambda_2}(s,\Omega) Y_{J,\lambda_1-\lambda_2}(\Omega)$$

EWSBS partial waves

The form of the partial wave is

$$A_{IJ}(s) = A_{IJ}^{(0)} + A_{IJ}^{(1)} + \mathcal{O}\left[(s/v^2)^3\right].$$

Which will be decomposed as

$$A_{IJ}^{(0)} = Ks$$
$$A_{IJ}^{(1)} = \left(B(\mu) + D\log\frac{s}{\mu^2} + E\log\frac{-s}{\mu^2}\right)s^2.$$

As $A_{IJ}(s)$ must be scale independent,

$$B(\mu) = B(\mu_0) + (D+E)\log\frac{\mu^2}{\mu_0^2}$$
$$= B_0 + p_4 a_4(\mu) + p_5 a_5(\mu).$$

EWSBS partial waves

The form of the partial wave is

$$A_{IJ}(s) = A_{IJ}^{(0)} + A_{IJ}^{(1)} + \mathcal{O}\left[(s/v^2)^3\right].$$

Which will be decomposed as

$$\begin{aligned} A_{IJ}^{(0)} &= Ks \\ A_{IJ}^{(1)} &= \left(B(\mu) + D\log\frac{s}{\mu^2} + E\log\frac{-s}{\mu^2}\right)s^2. \end{aligned}$$

As $A_{IJ}(s)$ must be scale independent,

$$\begin{aligned} B(\mu) &= B(\mu_0) + (D+E)\log\frac{\mu^2}{\mu_0^2} \\ &= B_0 + p_4 a_4(\mu) + p_5 a_5(\mu). \end{aligned}$$

EWSBS partial waves

The form of the partial wave is

$$A_{IJ}(s) = A_{IJ}^{(0)} + A_{IJ}^{(1)} + \mathcal{O}\left[(s/v^2)^3\right].$$

Which will be decomposed as

$$\begin{aligned} A_{IJ}^{(0)} &= Ks \\ A_{IJ}^{(1)} &= \left(B(\mu) + D\log\frac{s}{\mu^2} + E\log\frac{-s}{\mu^2}\right)s^2. \end{aligned}$$

As $A_{IJ}(s)$ must be scale independent,

$$\begin{aligned} B(\mu) &= B(\mu_0) + (D+E)\log\frac{\mu^2}{\mu_0^2} \\ &= B_0 + p_4 a_4(\mu) + p_5 a_5(\mu). \end{aligned}$$

Partial wave decomposition: $\gamma\gamma$ states

The form of the partial wave is

$$P_{IJ,\Lambda}(s) = P^{(0)}_{IJ,\Lambda} + \mathcal{O}(\alpha_{\rm em}^2) + \mathcal{O}(\alpha_{\rm em} s^2).$$

Note that $\gamma\gamma$ with $J=2$, $\Lambda=\pm 2$ also couples with the EWSBS, following

$$P^{(0)}_{I0,0} \propto \alpha s \qquad\qquad P^{(0)}_{I2,\pm 2} \propto \alpha$$

- Based on a collaboration with profs. M.J.Herrero and J.J.Sanz-Cillero: JHEP**1407** (2014) 149.
- Partial waves, unitarization and study of the parameter space: Eur.Phys.J. C**77** (2017) no.4, 205.

Partial wave decomposition: $\gamma\gamma$ states

The form of the partial wave is

$$P_{IJ,\Lambda}(s) = P^{(0)}_{IJ,\Lambda} + \mathcal{O}(\alpha_{\rm em}^2) + \mathcal{O}(\alpha_{\rm em} s^2).$$

Note that $\gamma\gamma$ with $J = 2$, $\Lambda = \pm 2$ also couples with the EWSBS, following

$$P^{(0)}_{I0,0} \propto \alpha s \qquad\qquad P^{(0)}_{I2,\pm 2} \propto \alpha$$

- Based on a collaboration with profs. M.J.Herrero and J.J.Sanz-Cillero: JHEP**1407** (2014) 149.
- Partial waves, unitarization and study of the parameter space: Eur.Phys.J. C**77** (2017) no.4, 205.

Partial wave decomposition: $\gamma\gamma$ states

The form of the partial wave is

$$P_{IJ,\Lambda}(s) = P^{(0)}_{IJ,\Lambda} + \mathcal{O}(\alpha_{\rm em}^2) + \mathcal{O}(\alpha_{\rm em} s^2).$$

Note that $\gamma\gamma$ with $J = 2$, $\Lambda = \pm 2$ also couples
with the EWSBS, following

$$P^{(0)}_{I0,0} \propto \alpha s \qquad\qquad P^{(0)}_{I2,\pm 2} \propto \alpha$$

- Based on a collaboration with profs. M.J.Herrero and J.J.Sanz-Cillero: JHEP**1407** (2014) 149.
- Partial waves, unitarization and study of the parameter space: Eur.Phys.J. C**77** (2017) no.4, 205.

Partial wave decomposition: $t\bar{t}$ states

The form of the partial wave is

$$Q_{IJ}(s) = Q_{IJ}^{(0)} + Q_{IJ}^{(1)} + \mathcal{O}\left[M_t s^2 \sqrt{s}/v^6\right] + \mathcal{O}\left[M_t^2 s/v^4\right],$$

which will be decomposed as

$$Q_{IJ}^{(0)} = K^Q \sqrt{s} M_t$$
$$Q_{IJ}^{(1)} = \left(B^Q(\mu) + E^Q \log\frac{-s}{\mu^2}\right) s\sqrt{s} M_t.$$

As $A_{IJ}(s)$ must be scale independent,

$$B^Q(\mu) = B^Q(\mu_0) + E^Q \log\frac{\mu^2}{\mu_0^2}$$
$$= B_0 + p_g g_t(\mu).$$

- Based on a collaboration with A.Castillo: arXiv:1607.01158 [hep-ph], accepted in EPJC.

Partial wave decomposition: $t\bar{t}$ states

The form of the partial wave is

$$Q_{IJ}(s) = Q_{IJ}^{(0)} + Q_{IJ}^{(1)} + \mathcal{O}\left[M_t s^2 \sqrt{s}/v^6\right] + \mathcal{O}\left[M_t^2 s/v^4\right],$$

which will be decomposed as

$$\begin{aligned} Q_{IJ}^{(0)} &= K^Q \sqrt{s} M_t \\ Q_{IJ}^{(1)} &= \left(B^Q(\mu) + E^Q \log\frac{-s}{\mu^2}\right) s\sqrt{s} M_t. \end{aligned}$$

As $A_{IJ}(s)$ must be scale independent,

$$\begin{aligned} B^Q(\mu) &= B^Q(\mu_0) + E^Q \log\frac{\mu^2}{\mu_0^2} \\ &= B_0 + p_g g_t(\mu). \end{aligned}$$

- Based on a collaboration with A.Castillo: arXiv:1607.01158 [hep-ph], accepted in EPJC.

Partial wave decomposition: $t\bar{t}$ states

The form of the partial wave is

$$Q_{IJ}(s) = Q_{IJ}^{(0)} + Q_{IJ}^{(1)} + \mathcal{O}\left[M_t s^2 \sqrt{s}/v^6\right] + \mathcal{O}\left[M_t^2 s/v^4\right],$$

which will be decomposed as

$$\begin{aligned} Q_{IJ}^{(0)} &= K^Q \sqrt{s} M_t \\ Q_{IJ}^{(1)} &= \left(B^Q(\mu) + E^Q \log \frac{-s}{\mu^2}\right) s\sqrt{s} M_t. \end{aligned}$$

As $A_{IJ}(s)$ must be scale independent,

$$\begin{aligned} B^Q(\mu) &= B^Q(\mu_0) + E^Q \log \frac{\mu^2}{\mu_0^2} \\ &= B_0 + p_g g_t(\mu). \end{aligned}$$

- Based on a collaboration with A.Castillo: arXiv:1607.01158 [hep-ph], accepted in EPJC.

Partial wave decomposition: $t\bar{t}$ states

The form of the partial wave is

$$Q_{IJ}(s) = Q_{IJ}^{(0)} + Q_{IJ}^{(1)} + \mathcal{O}\left[M_t s^2 \sqrt{s}/v^6\right] + \mathcal{O}\left[M_t^2 s/v^4\right],$$

which will be decomposed as

$$Q_{IJ}^{(0)} = K^Q \sqrt{s} M_t$$
$$Q_{IJ}^{(1)} = \left(B^Q(\mu) + E^Q \log\frac{-s}{\mu^2}\right) s\sqrt{s} M_t.$$

As $A_{IJ}(s)$ must be scale independent,

$$B^Q(\mu) = B^Q(\mu_0) + E^Q \log\frac{\mu^2}{\mu_0^2}$$
$$= B_0 + p_g g_t(\mu).$$

- Based on a collaboration with A.Castillo: arXiv:1607.01158 [hep-ph], accepted in EPJC.

Unitarity for partial waves

- Unit. cond. for $S - matrix$: $SS^\dagger = \mathbb{1}$,
- plus analytical properties of matrix elements,
- plus time reversal invariance,

Unitarity condition for partial waves

$$\mathrm{Im}\, A_{IJ,p_i\to k_1}(s) = \sum_{\{a,b\}} \sqrt{1-\frac{4m_q^2}{s}}[A_{IJ,p_i\to q_{i,ab}}(s)][A_{IJ,q_{i,ab}\to k_i}(s)]^*$$

Unitarity for partial waves

- Unit. cond. for $S - matrix$: $SS^\dagger = \mathbb{1}$,
- plus analytical properties of matrix elements,
- plus time reversal invariance,

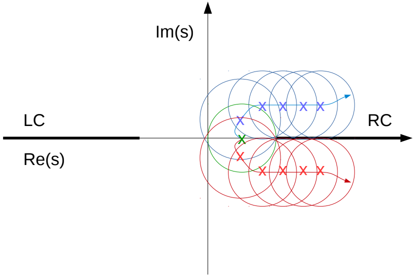

Unitarity condition for partial waves

$$\operatorname{Im} A_{IJ,p_i \to k_1}(s) = \sum_{\{a,b\}} \sqrt{1 - \frac{4m_q^2}{s}} [A_{IJ,p_i \to q_{i,ab}}(s)][A_{IJ,q_{i,ab} \to k_i}(s)]^*$$

Unitarity for partial waves

- Unit. cond. for $S-matrix$: $SS^{\dagger} = \mathbb{1}$,
- plus analytical properties of matrix elements,
- plus time reversal invariance,

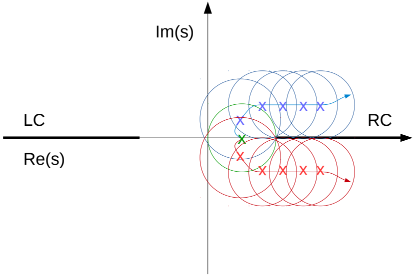

Unitarity condition for partial waves

$$\mathrm{Im}\, A_{IJ,p_i\to k_1}(s) = \sum_{\{a,b\}} \sqrt{1-\frac{4m_q^2}{s}}[A_{IJ,p_i\to q_{i,ab}}(s)][A_{IJ,q_{i,ab}\to k_i}(s)]^*$$

Unitarity for partial waves

- Unit. cond. for $S - matrix$: $SS^\dagger = \mathbb{1}$,
- plus analytical properties of matrix elements,
- plus time reversal invariance,

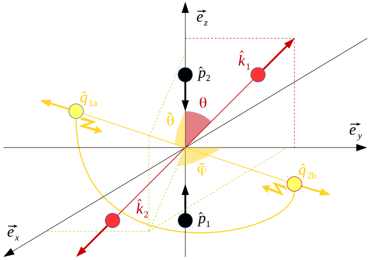

Unitarity condition for partial waves

$$\mathrm{Im}\, A_{IJ,p_i\to k_1}(s) = \sum_{\{a,b\}} \sqrt{1 - \frac{4m_q^2}{s}} [A_{IJ,p_i\to q_{i,ab}}(s)][A_{IJ,q_{i,ab}\to k_i}(s)]^*$$

Unitarization procedures for elastic processes

$$A^{IAM}(s) = \frac{[A^{(0)}(s)]^2}{A^{(0)}(s) - A^{(1)}(s)},$$

$$A^{N/D}(s) = \frac{A^{(0)}(s) + A_L(s)}{1 - \frac{A_R(s)}{A^{(0)}(s)} + \frac{1}{2}g(s)A_L(-s)},$$

$$A^{IK}(s) = \frac{A^{(0)}(s) + A_L(s)}{1 - \frac{A_R(s)}{A^{(0)}(s)} + g(s)A_L(s)},$$

$$A_0^K(s) = \frac{A_0(s)}{1 - iA_0(s)},$$

where

$$g(s) = \frac{1}{\pi}\left(\frac{B(\mu)}{D+E} + \log\frac{-s}{\mu^2}\right)$$

$$A_L(s) = \pi g(-s) D s^2$$

$$A_R(s) = \pi g(s) E s^2$$

PRD **91** (2015) 075017

Unitarization procedures for elastic processes

$$A^{IAM}(s) = \frac{[A^{(0)}(s)]^2}{A^{(0)}(s) - A^{(1)}(s)},$$

$$A^{N/D}(s) = \frac{A^{(0)}(s) + A_L(s)}{1 - \frac{A_R(s)}{A^{(0)}(s)} + \frac{1}{2}g(s)A_L(-s)},$$

$$A^{IK}(s) = \frac{A^{(0)}(s) + A_L(s)}{1 - \frac{A_R(s)}{A^{(0)}(s)} + g(s)A_L(s)},$$

$$A_0^K(s) = \frac{A_0(s)}{1 - iA_0(s)},$$

where

$$g(s) = \frac{1}{\pi}\left(\frac{B(\mu)}{D+E} + \log\frac{-s}{\mu^2}\right)$$

$$A_L(s) = \pi g(-s) D s^2$$

$$A_R(s) = \pi g(s) E s^2$$

PRD **91** (2015) 075017

Unitarization procedures for elastic processes

$$A^{IAM}(s) = \frac{[A^{(0)}(s)]^2}{A^{(0)}(s) - A^{(1)}(s)},$$

$$A^{N/D}(s) = \frac{A^{(0)}(s) + A_L(s)}{1 - \frac{A_R(s)}{A^{(0)}(s)} + \frac{1}{2}g(s)A_L(-s)},$$

$$A^{IK}(s) = \frac{A^{(0)}(s) + A_L(s)}{1 - \frac{A_R(s)}{A^{(0)}(s)} + g(s)A_L(s)},$$

$$A_0^K(s) = \frac{A_0(s)}{1 - iA_0(s)},$$

where

$$g(s) = \frac{1}{\pi}\left(\frac{B(\mu)}{D+E} + \log\frac{-s}{\mu^2}\right)$$

$$A_L(s) = \pi g(-s) D s^2$$

$$A_R(s) = \pi g(s) E s^2$$

PRD **91** (2015) 075017

Unitarization procedures for elastic processes

$$A^{IAM}(s) = \frac{[A^{(0)}(s)]^2}{A^{(0)}(s) - A^{(1)}(s)},$$

$$A^{N/D}(s) = \frac{A^{(0)}(s) + A_L(s)}{1 - \frac{A_R(s)}{A^{(0)}(s)} + \frac{1}{2}g(s)A_L(-s)},$$

$$A^{IK}(s) = \frac{A^{(0)}(s) + A_L(s)}{1 - \frac{A_R(s)}{A^{(0)}(s)} + g(s)A_L(s)},$$

$$A_0^K(s) = \frac{A_0(s)}{1 - iA_0(s)},$$

where

$$g(s) = \frac{1}{\pi}\left(\frac{B(\mu)}{D+E} + \log\frac{-s}{\mu^2}\right)$$

$$A_L(s) = \pi g(-s) D s^2$$

$$A_R(s) = \pi g(s) E s^2$$

PRD **91** (2015) 075017

Matricial versions of the methods

$$F^{IAM}(s) = \left[F^{(0)}(s)\right]^{-1} \cdot \left[F^{(0)}(s) - F^{(1)}(s)\right] \cdot \left[F^{(0)}(s)\right]^{-1},$$

$$F^{N/D}(s) = \left[1 - F_R(s) \cdot \left(F^{(0)}(s)\right)^{-1} + \frac{1}{2} G(s) F_L(-s)\right]^{-1} \cdot N_0(s),$$

$$F^{IK}(s) = [1 + G(s) \cdot N_0(s)]^{-1} \cdot N_0(s),$$

where $G(s)$, $F_L(s)$, $F_R(s)$ and $N_0(s)$ are defined as

$$G(s) = \frac{1}{\pi}\left(B(\mu)(D+E)^{-1} + \log\frac{-s}{\mu^2}\right)$$

$$F_L(s) = \pi G(-s) D s^2$$

$$F_R(s) = \pi G(s) E s^2$$

$$N_0(s) = F^{(0)}(s) + F_L(s)$$

PRD **91** (2015) 075017

Matricial versions of the methods

$$F^{IAM}(s) = \left[F^{(0)}(s)\right]^{-1} \cdot \left[F^{(0)}(s) - F^{(1)}(s)\right] \cdot \left[F^{(0)}(s)\right]^{-1},$$

$$F^{N/D}(s) = \left[1 - F_R(s) \cdot \left(F^{(0)}(s)\right)^{-1} + \frac{1}{2} G(s) F_L(-s)\right]^{-1} \cdot N_0(s),$$

$$F^{IK}(s) = [1 + G(s) \cdot N_0(s)]^{-1} \cdot N_0(s),$$

where $G(s)$, $F_L(s)$, $F_R(s)$ and $N_0(s)$ are defined as

$$G(s) = \frac{1}{\pi}\left(B(\mu)(D+E)^{-1} + \log\frac{-s}{\mu^2}\right)$$

$$F_L(s) = \pi G(-s) D s^2$$

$$F_R(s) = \pi G(s) E s^2$$

$$N_0(s) = F^{(0)}(s) + F_L(s)$$

PRD **91** (2015) 075017

Matricial versions of the methods

$$F^{IAM}(s) = \left[F^{(0)}(s)\right]^{-1} \cdot \left[F^{(0)}(s) - F^{(1)}(s)\right] \cdot \left[F^{(0)}(s)\right]^{-1},$$

$$F^{N/D}(s) = \left[1 - F_R(s) \cdot \left(F^{(0)}(s)\right)^{-1} + \frac{1}{2} G(s) F_L(-s)\right]^{-1} \cdot N_0(s),$$

$$F^{IK}(s) = [1 + G(s) \cdot N_0(s)]^{-1} \cdot N_0(s),$$

where $G(s)$, $F_L(s)$, $F_R(s)$ and $N_0(s)$ are defined as

$$G(s) = \frac{1}{\pi}\left(B(\mu)(D+E)^{-1} + \log\frac{-s}{\mu^2}\right)$$

$$F_L(s) = \pi G(-s) D s^2$$

$$F_R(s) = \pi G(s) E s^2$$

$$N_0(s) = F^{(0)}(s) + F_L(s)$$

PRD **91** (2015) 075017

Extension to $\gamma\gamma$ and $t\bar{t}$ scattering

Basic assumption

- EWSBS is strongly interacting. $\gamma\gamma$ and $t\bar{t}$ are perturbative.
- Coupling with photons, controlled by $\alpha = e^2/4\pi \ll s/v^2$.
- Coupling with top quarks, controlled by $M_t\sqrt{s}/v^2 \ll s/v^2$.

Perturbative unitarization: $\omega\omega \to \{\gamma\gamma, t\bar{t}\}$

$$\tilde{P} = \frac{\tilde{A}_{IJ}}{A_{IJ}^{(0)}} P^{(0)}$$

Perturbative unitarization: $\{\omega\omega, hh\} \to \{\gamma\gamma, t\bar{t}\}$

$$\begin{pmatrix} \tilde{P} \\ \tilde{R} \end{pmatrix} = \tilde{F} \left(F^{(0)}\right)^{-1} \begin{pmatrix} P^{(0)} \\ R^{(0)} \end{pmatrix}$$

Extension to $\gamma\gamma$ and $t\bar{t}$ scattering

Basic assumption

- EWSBS is strongly interacting. $\gamma\gamma$ and $t\bar{t}$ are perturbative.
- Coupling with photons, controlled by $\alpha = e^2/4\pi \ll s/v^2$.
- Coupling with top quarks, controlled by $M_t\sqrt{s}/v^2 \ll s/v^2$.

Perturbative unitarization: $\omega\omega \to \{\gamma\gamma, t\bar{t}\}$

$$\tilde{P} = \frac{\tilde{A}_{IJ}}{A_{IJ}^{(0)}} P^{(0)}$$

Perturbative unitarization: $\{\omega\omega, hh\} \to \{\gamma\gamma, t\bar{t}\}$

$$\begin{pmatrix} \tilde{P} \\ \tilde{R} \end{pmatrix} = \tilde{F} \left(F^{(0)}\right)^{-1} \begin{pmatrix} P^{(0)} \\ R^{(0)} \end{pmatrix}$$

Extension to $\gamma\gamma$ and $t\bar{t}$ scattering

Basic assumption

- EWSBS is strongly interacting. $\gamma\gamma$ and $t\bar{t}$ are perturbative.
- Coupling with photons, controlled by $\alpha = e^2/4\pi \ll s/v^2$.
- Coupling with top quarks, controlled by $M_t\sqrt{s}/v^2 \ll s/v^2$.

Perturbative unitarization: $\omega\omega \to \{\gamma\gamma, t\bar{t}\}$

$$\tilde{P} = \frac{\tilde{A}_{IJ}}{A_{IJ}^{(0)}} P^{(0)}$$

Perturbative unitarization: $\{\omega\omega, hh\} \to \{\gamma\gamma, t\bar{t}\}$

$$\begin{pmatrix} \tilde{P} \\ \tilde{R} \end{pmatrix} = \tilde{F} \left(F^{(0)}\right)^{-1} \begin{pmatrix} P^{(0)} \\ R^{(0)} \end{pmatrix}$$

Extension to $\gamma\gamma$ and $t\bar{t}$ scattering

Basic assumption

- EWSBS is strongly interacting. $\gamma\gamma$ and $t\bar{t}$ are perturbative.
- Coupling with photons, controlled by $\alpha = e^2/4\pi \ll s/v^2$.
- Coupling with top quarks, controlled by $M_t\sqrt{s}/v^2 \ll s/v^2$.

Perturbative unitarization: $\omega\omega \to \{\gamma\gamma, t\bar{t}\}$

$$\tilde{P} = \frac{\tilde{A}_{IJ}}{A_{IJ}^{(0)}} P^{(0)}$$

Perturbative unitarization: $\{\omega\omega, hh\} \to \{\gamma\gamma, t\bar{t}\}$

$$\begin{pmatrix} \tilde{P} \\ \tilde{R} \end{pmatrix} = \tilde{F}\left(F^{(0)}\right)^{-1}\begin{pmatrix} P^{(0)} \\ R^{(0)} \end{pmatrix}$$

Extension to $\gamma\gamma$ and $t\bar{t}$ scattering

Basic assumption

- EWSBS is strongly interacting. $\gamma\gamma$ and $t\bar{t}$ are perturbative.
- Coupling with photons, controlled by $\alpha = e^2/4\pi \ll s/v^2$.
- Coupling with top quarks, controlled by $M_t\sqrt{s}/v^2 \ll s/v^2$.

Perturbative unitarization: $\omega\omega \to \{\gamma\gamma, t\bar{t}\}$

$$\tilde{P} = \frac{\tilde{A}_{IJ}}{A_{IJ}^{(0)}} P^{(0)}$$

Perturbative unitarization: $\{\omega\omega, hh\} \to \{\gamma\gamma, t\bar{t}\}$

$$\begin{pmatrix} \tilde{P} \\ \tilde{R} \end{pmatrix} = \tilde{F}\left(F^{(0)}\right)^{-1}\begin{pmatrix} P^{(0)} \\ R^{(0)} \end{pmatrix}$$

Usability channel of unitarization procedures

IJ	00	02	11	20	22
Method of choice	Any	N/D IK	IAM	Any	N/D IK

- The IAM method cannot be used when $A^{(0)} = 0$, because it would give a vanishing value.
- The N/D and the IK methods cannot be used if $D + E = 0$, because in this case computing $A_L(s)$ and $A_R(s)$ is not possible.
- The naive K-matrix method,

$$A_0^K(s) = \frac{A_0(s)}{1 - iA_0(s)},$$

fails because it is not analytical in the first Riemann sheet and, consequently, it is not a proper partial wave compatible with microcausality.

Usability channel of unitarization procedures

IJ	00	02	11	20	22
Method of choice	Any	N/D IK	IAM	Any	N/D IK

- The IAM method cannot be used when $A^{(0)} = 0$, because it would give a vanishing value.
- The N/D and the IK methods cannot be used if $D + E = 0$, because in this case computing $A_L(s)$ and $A_R(s)$ is not possible.
- The naive K-matrix method,

$$A_0^K(s) = \frac{A_0(s)}{1 - iA_0(s)},$$

fails because it is not analytical in the first Riemann sheet and, consequently, it is not a proper partial wave compatible with microcausality.

Usability channel of unitarization procedures

IJ	00	02	11	20	22
Method of choice	Any	N/D IK	IAM	Any	N/D IK

- The IAM method cannot be used when $A^{(0)} = 0$, because it would give a vanishing value.
- The N/D and the IK methods cannot be used if $D + E = 0$, because in this case computing $A_L(s)$ and $A_R(s)$ is not possible.
- The naive K-matrix method,

$$A_0^K(s) = \frac{A_0(s)}{1 - iA_0(s)},$$

fails because it is not analytical in the first Riemann sheet and, consequently, it is not a proper partial wave compatible with microcausality.

Scalar-isoscalar channels

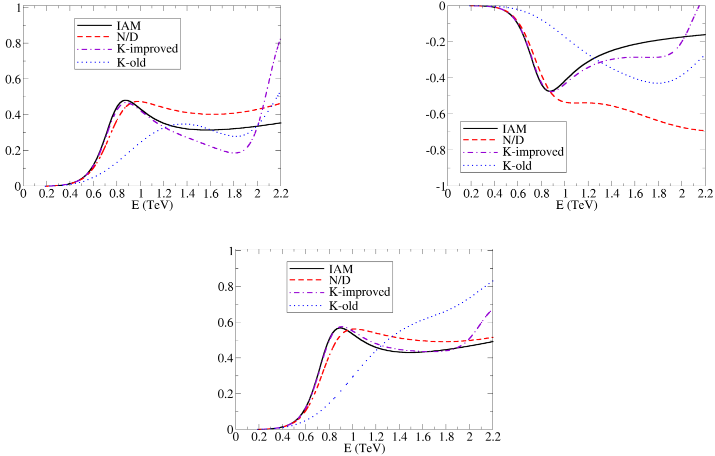

From left to right and top to bottom, elastic $\omega\omega$, elastic hh, and cross channel $\omega\omega \to hh$, for $a = 0.88$, $b = 3$, $\mu = 3\,\mathrm{TeV}$ and all NLO parameters set to 0.
PRL **114** (2015) 221803, PRD **91** (2015) 075017.

Vector-isovector channels

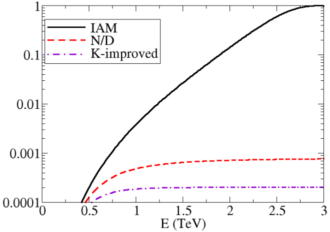

From our ref[12]. We have taken $a = 0.88$ and $b = 1.5$, but while for the left plot all the NLO parameters vanish, for the right plot we have taken $a_4 = 0.003$, known to yield an IAM resonance according to the Barcelona group[13].

---

[12] PRD **91** (2015) 075017
[13] PRD **90** (2014) 015035

Scalar-isotensor channels ($IJ = 20$)

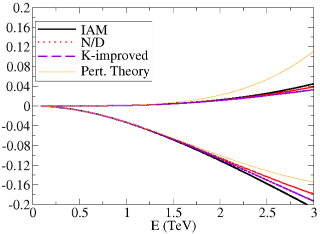

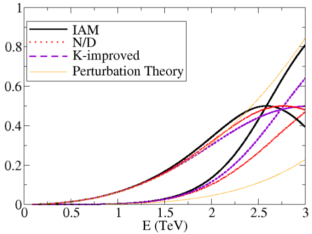

From our ref[14]. From left to right, $a = 0.88$, $a = 1.15$. We have taken $b = a^2$ and the NLO parameters set to zero. Both real and imaginary part shown. Real ones correspond to bottom lines at left and upper at low E at right.

[14] PRD **91** (2015) 075017

Isotensor-scalar channels ($IJ = 02$)

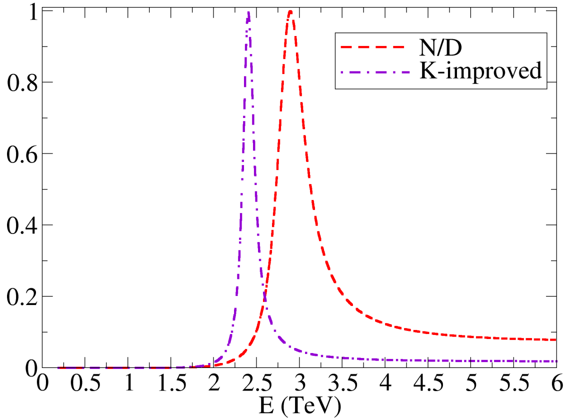

$a = 0.88$, $b = a^2$, $a_4 = -2a_5 = 3/(192\pi)$, all the other NLO param. set to zero. PRD **91** (2015) 075017.

Reson. in $W_L W_L \to W_L W_L$ due to a_4 and a_5, ours

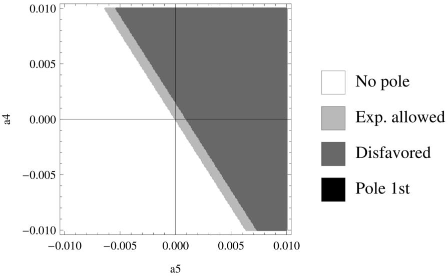

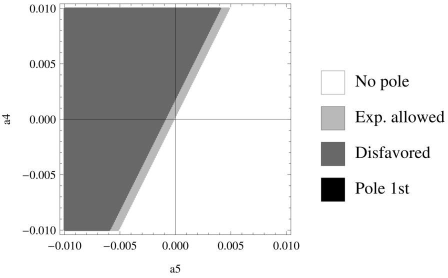

- $a = 0.90,\ b = a^2$
  PRD **91** (2015) 075017
- From left, clockwise,
  $IJ = 00,\ 11,\ 20$
- Excluding resonances
  $M_S < 700\,\mathrm{GeV},\ M_V < 1.5\,\mathrm{TeV}$

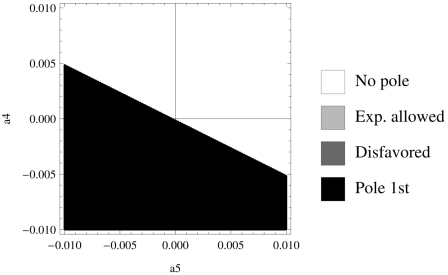

Reson. in $W_L W_L \to W_L W_L$ due to a_4 and a_5, Barcelona

CROSS-CHECK: Espriu, Yencho, Mescia
PRD**88**, 055002
PRD**90**, 015035
At right, exclusion regions include resonances with $M_{S,V} < 600\,\mathrm{GeV}$.

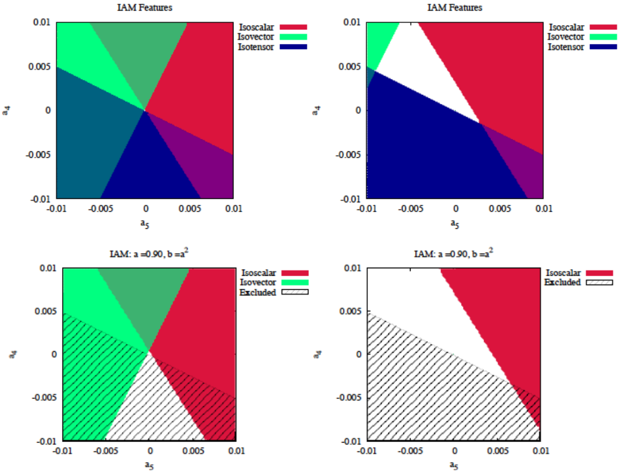

Resonance from $W_L W_L \to hh$

$a = 1,\ b = 2$, IAM,
elastic chann. $W_L W_L \to W_L W_L$,
red figure from 3D-printer

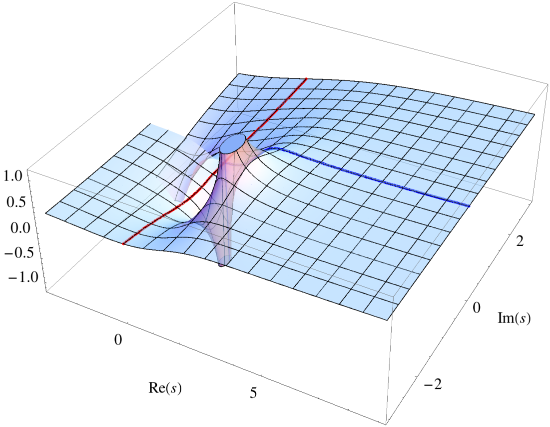

Rafael L. Delgado,
Antonio Dobado,
Felipe J. Llanes-Estrada,
Possible New Resonance from W_L W_L-hh Interchannel Coupling,

PRL **114** (2015) 221803

Resonance from $W_L W_L \to hh$

$a = 1,\ b = 2$, IAM,
inelastic chann. $W_L W_L \to hh$,
yellow figure from 3D-printer

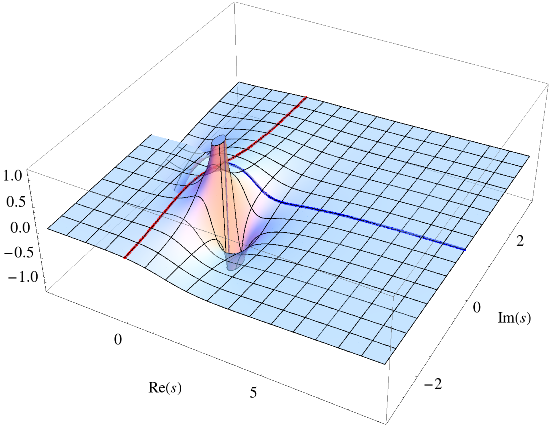

Rafael L. Delgado,
Antonio Dobado,
Felipe J. Llanes-Estrada,
Possible New Resonance from W_L W_L-hh Interchannel Coupling,

PRL **114** (2015) 221803

Resonances in $W_L W_L \to W_L W_L$ due to a and b parameters

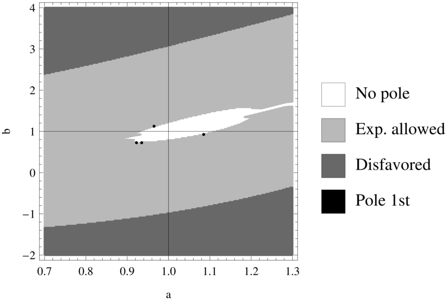

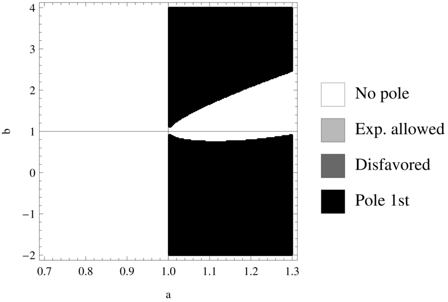

- PRL & PRD **91** (2015) 075017
- From left, clockwise, $IJ = 00,\ 11,\ 20$
- Excluding resonances $M_S < 700\,\mathrm{GeV}$, $M_V < 1.5\,\mathrm{TeV}$
- Constraint over b even without data about $W_L W_L \to hh$ and $hh \to hh$ scattering processes.

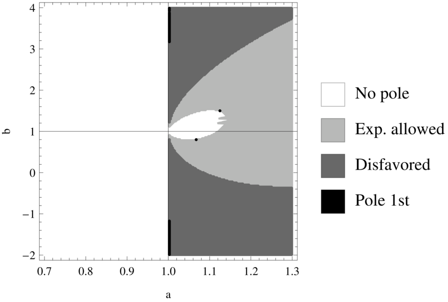

Motion of the resonance mass and width

Dependence on b with $a^2 = 1$ fixed (upper curve) and for $a = 1 - \xi$ and $b = 1 - 2\xi$ with $\xi = v/f$ as in the MCHM (lower blue curve).

PRL **114** (2015) 221803

Video,
(a,b) param. space

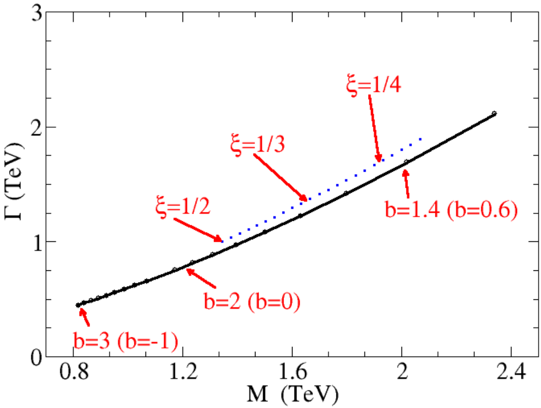

Resonances in $W_L W_L \to W_L W_L$ due to a and a_4 parameters

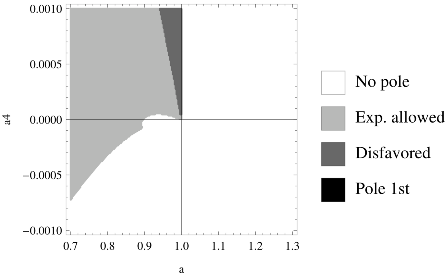

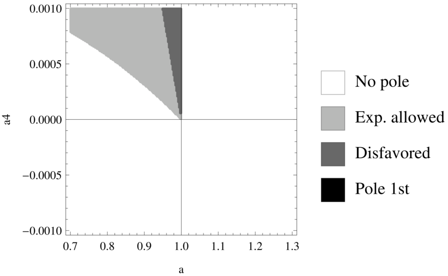

- $b = a^2$
  PRD **91** (2015) 075017
- From left, clockwise,
  $IJ = 00,\ 11,\ 20$
- Excluding resonances
  $M_S < 700\,\mathrm{GeV},\ M_V < 1.5\,\mathrm{TeV}$

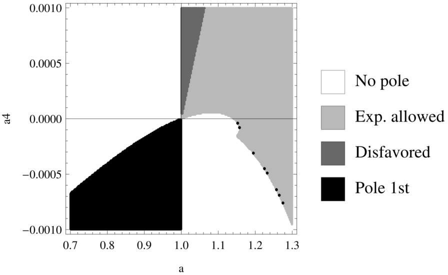

Resonances in $W_L W_L \to W_L W_L$ due to b, g, d and e parameters

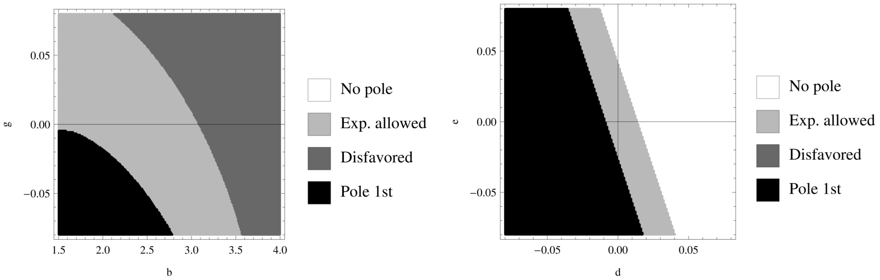

Effective Theory, PRD **91** (2015) 075017, isoscalar channels ($I = J = 0$).

I) IAM method

This method needs a NLO computation,

$$\tilde{t}^\omega = \frac{t_0^\omega}{1 - \frac{t_1^\omega}{t_0^\omega}},$$

where

$$t_1^\omega = s^2\left(D\log\left[\frac{s}{\mu^2}\right] + E\log\left[\frac{-s}{\mu^2}\right] + (D+E)\log\left[\frac{\mu^2}{\mu_0^2}\right]\right)$$

I) IAM method

This method needs a NLO computation,

$$\tilde{t}^{\omega} = \frac{t_0^{\omega}}{1 - \frac{t_1^{\omega}}{t_0^{\omega}}},$$

where

$$t_1^{\omega} = s^2 \left(D \log\left[\frac{s}{\mu^2}\right] + E \log\left[\frac{-s}{\mu^2}\right] + (D+E) \log\left[\frac{\mu^2}{\mu_0^2}\right] \right)$$

Check at tree level

We have checked[15], for the tree level case,

$$\mathcal{L} = \frac{1}{2}g(\varphi/f)\partial_\mu\omega^a\partial^\mu\omega^b\left(\delta_{ab}+\frac{\omega^a\omega^b}{v^2-\omega^2}\right)$$
$$+\frac{1}{2}\partial_\mu\varphi\partial^\mu\varphi-\frac{1}{2}M_\varphi^2\varphi^2-\lambda_3\varphi^3-\lambda_4\varphi^4+\dots$$
$$g(\varphi/f) = 1+\sum_{n=1}^{\infty}g_n\left(\frac{\varphi}{f}\right)^n = 1+2\alpha\frac{\varphi}{f}+\beta\left(\frac{\varphi}{f}\right)^2+..$$

where $a\equiv\alpha v/f$, $b=\beta v^2/f^2$, and so one, the concordance with the methods

[15] See J.Phys. G41 (2014) 025002.

Check at tree level

We have checked[15], for the tree level case,

$$\begin{aligned}\mathcal{L} &= \frac{1}{2}g(\varphi/f)\partial_\mu\omega^a\partial^\mu\omega^b\left(\delta_{ab}+\frac{\omega^a\omega^b}{v^2-\omega^2}\right)\\ &+\frac{1}{2}\partial_\mu\varphi\partial^\mu\varphi-\frac{1}{2}M_\varphi^2\varphi^2-\lambda_3\varphi^3-\lambda_4\varphi^4+\ldots\\ g(\varphi/f) &= 1+\sum_{n=1}^{\infty}g_n\left(\frac{\varphi}{f}\right)^n=1+2\alpha\frac{\varphi}{f}+\beta\left(\frac{\varphi}{f}\right)^2+..\end{aligned}$$

where $a\equiv\alpha v/f$, $b=\beta v^2/f^2$, and so one, the concordance with the methods

[15] See J.Phys. G41 (2014) 025002.

Check at tree level

We have checked[15], for the tree level case,

$$\begin{aligned}\mathcal{L} &= \frac{1}{2}g(\varphi/f)\partial_\mu\omega^a\partial^\mu\omega^b\left(\delta_{ab}+\frac{\omega^a\omega^b}{v^2-\omega^2}\right)\\ &\quad +\frac{1}{2}\partial_\mu\varphi\partial^\mu\varphi-\frac{1}{2}M_\varphi^2\varphi^2-\lambda_3\varphi^3-\lambda_4\varphi^4+\dots\\ g(\varphi/f) &= 1+\sum_{n=1}^{\infty}g_n\left(\frac{\varphi}{f}\right)^n = 1+2\alpha\frac{\varphi}{f}+\beta\left(\frac{\varphi}{f}\right)^2+..\end{aligned}$$

where $a\equiv\alpha v/f$, $b=\beta v^2/f^2$, and so one, the concordance with the methods

[15] See J.Phys. G41 (2014) 025002.

Check at tree level

We have checked[15], for the tree level case,

$$\begin{aligned}\mathcal{L} &= \frac{1}{2}g(\varphi/f)\partial_\mu\omega^a\partial^\mu\omega^b\left(\delta_{ab}+\frac{\omega^a\omega^b}{v^2-\omega^2}\right)\\ &\quad+\frac{1}{2}\partial_\mu\varphi\partial^\mu\varphi-\frac{1}{2}M_\varphi^2\varphi^2-\lambda_3\varphi^3-\lambda_4\varphi^4+\ldots\\ g(\varphi/f) &= 1+\sum_{n=1}^{\infty}g_n\left(\frac{\varphi}{f}\right)^n=1+2\alpha\frac{\varphi}{f}+\beta\left(\frac{\varphi}{f}\right)^2+..\end{aligned}$$

where $a\equiv\alpha v/f$, $b=\beta v^2/f^2$, and so one, the concordance with the methods

[15] See J.Phys. G41 (2014) 025002.

II) K matrix

$$\tilde{T} = T(1 - J(s)T)^{-1}, \quad , J(s) = -\frac{1}{\pi}\log\left[\frac{-s}{\Lambda^2}\right],$$

so that, for $\tilde{t}_\omega$,

$$\tilde{t}_\omega = \frac{t_\omega - J(t_\omega t_\varphi - t_{\omega\varphi}^2)}{1 - J(t_\omega + t_\varphi) + J^2(t_\omega t_\varphi - t_{\omega\varphi}^2)},$$

for $\beta = \alpha^2$ (elastic case),

$$\tilde{t}_\omega = \frac{t_\omega}{1 - Jt_\omega}$$

$$\tilde{T} = T(1 - J(s)T)^{-1}, \quad , J(s) = -\frac{1}{\pi}\log\left[\frac{-s}{\Lambda^2}\right],$$

so that, for $\tilde{t}_\omega$,

$$\tilde{t}_\omega = \frac{t_\omega - J(t_\omega t_\varphi - t_{\omega\varphi}^2)}{1 - J(t_\omega + t_\varphi) + J^2(t_\omega t_\varphi - t_{\omega\varphi}^2)},$$

for $\beta = \alpha^2$ (elastic case),

$$\tilde{t}_\omega = \frac{t_\omega}{1 - Jt_\omega}$$

II) K matrix

$$\tilde{T} = T(1 - J(s)T)^{-1}, \quad , J(s) = -\frac{1}{\pi}\log\left[\frac{-s}{\Lambda^2}\right],$$

so that, for $\tilde{t}_\omega$,

$$\tilde{t}_\omega = \frac{t_\omega - J(t_\omega t_\varphi - t_{\omega\varphi}^2)}{1 - J(t_\omega + t_\varphi) + J^2(t_\omega t_\varphi - t_{\omega\varphi}^2)},$$

for $\beta = \alpha^2$ (elastic case),

$$\tilde{t}_\omega = \frac{t_\omega}{1 - Jt_\omega}$$

$N \to \infty$, with v^2/N fixed. The amplitude A_N to order $1/N$ is a Lippmann-Schwinger series,

$$A_N = A - A\frac{NI}{2}A + A\frac{NI}{2}A\frac{NI}{2}A - \dots$$
$$I(s) = \int \frac{d^4q}{(2\pi)^4}\frac{i}{q^2(q+p)^2} = \frac{1}{16\pi^2}\log\left[\frac{-s}{\Lambda^2}\right] = -\frac{1}{8\pi}J(s)$$

Note: actually, $N = 3$. For the (iso)scalar partial wave (chiral limit, $I = J = 0$),

$$t_N^\omega(s) = \frac{t_0^\omega}{1 - Jt_0^\omega}$$

III)Large N

$N \to \infty$, with v^2/N fixed. The amplitude A_N to order $1/N$ is a Lippmann-Schwinger series,

$$A_N = A - A\frac{NI}{2}A + A\frac{NI}{2}A\frac{NI}{2}A - \dots$$
$$I(s) = \int \frac{d^4q}{(2\pi)^4}\frac{i}{q^2(q+p)^2} = \frac{1}{16\pi^2}\log\left[\frac{-s}{\Lambda^2}\right] = -\frac{1}{8\pi}J(s)$$

Note: actually, $N=3$. For the (iso)scalar partial wave (chiral limit, $I=J=0$),

$$t_N^\omega(s) = \frac{t_0^\omega}{1 - Jt_0^\omega}$$

III)Large N

$N \to \infty$, with v^2/N fixed. The amplitude A_N to order $1/N$ is a Lippmann-Schwinger series,

$$\begin{aligned} A_N &= A - A\frac{NI}{2}A + A\frac{NI}{2}A\frac{NI}{2}A - \dots \\ I(s) &= \int \frac{d^4q}{(2\pi)^4}\frac{i}{q^2(q+p)^2} = \frac{1}{16\pi^2}\log\left[\frac{-s}{\Lambda^2}\right] = -\frac{1}{8\pi}J(s) \end{aligned}$$

Note: actually, $N = 3$. For the (iso)scalar partial wave (chiral limit, $I = J = 0$),

$$t_N^\omega(s) = \frac{t_0^\omega}{1 - Jt_0^\omega}$$

IV) N/D

(elastic scattering at tree level only $\beta = \alpha^2$. See ref. J.Phys. G41 (2014) 025002). Ansatz

$$\tilde{t}^{\omega}(s) = \frac{N(s)}{D(s)},$$

where $N(s)$ has a left hand cut (and $\mathrm{Im}\, N(s > 0) = 0$)
$D(s)$ has a right hand cut (and $\Im D(s < 0) = 0$);

$$D(s) = 1 - \frac{s}{\pi}\int_0^{\infty} \frac{ds' N(s')}{s'(s' - s - i\epsilon)}$$

$$N(s) = \frac{s}{\pi}\int_{-\infty}^{0} \frac{ds' \,\mathrm{Im}\, N(s')}{s'(s' - s - i\epsilon)}$$

Coupled channels, tree level amplitudes

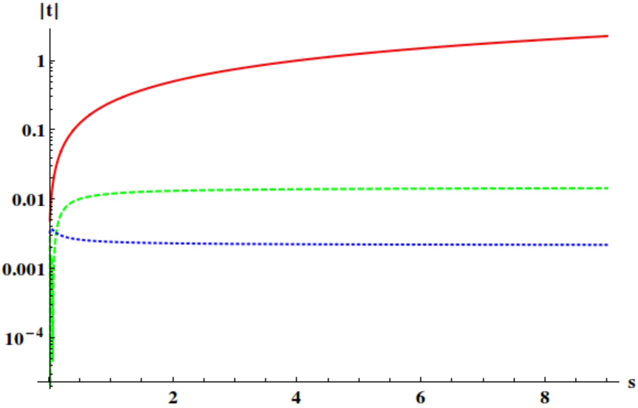

$f = 2v$, $\beta = \alpha^2 = 1$, $\lambda_3 = M_\varphi^2/f$, $\lambda_4 = M_\varphi^2/f^2$. OX axis: s in TeV^2.

Tree level, modulus of $\tilde{t}_\omega$, K matrix

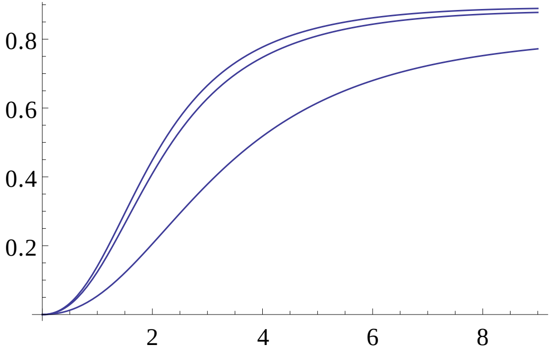

- All units in TeV.
- From top to bottom, $f = 1.2,\ 0.8,\ 0.4\,\mathrm{TeV}$
- $\Lambda = 3\,\mathrm{TeV}$
- $\mu = 100\,\mathrm{GeV}$

$\mathrm{Im}\, t_\omega$ in the N/D method, $f = 1\,\mathrm{TeV}$, $\beta = 1$, $m = 150\,\mathrm{GeV}$

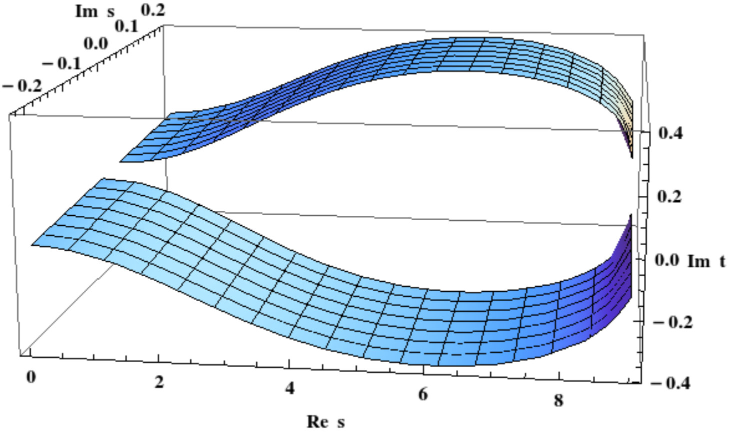

Re t_ω and Im t_ω, large N, $f = 400\,\mathrm{GeV}$

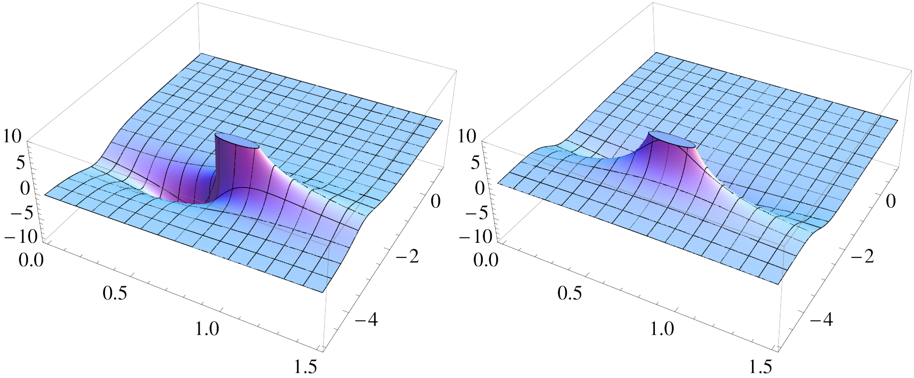

$\mathrm{Re}\, t_\omega$ and $\mathrm{Im}\, t_\omega$, large N, $f = 4\,\mathrm{TeV}$

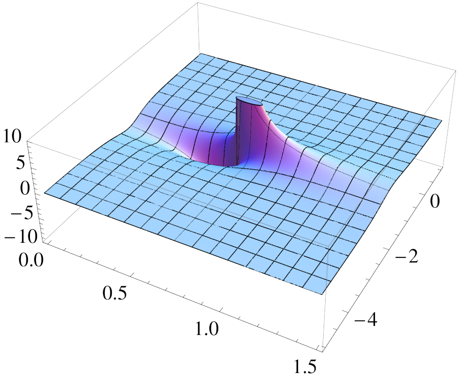

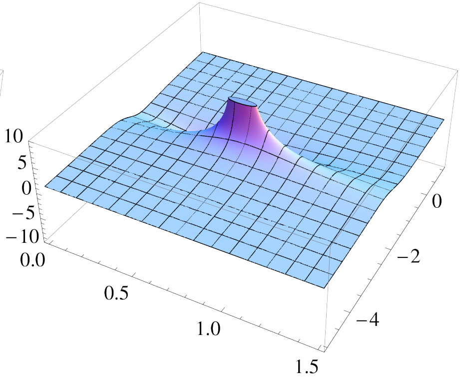

Tree level, motion of the pole position of t_ω
K–matrix, $M_\phi = 125\,\mathrm{GeV}$, $f \in (250\,\mathrm{GeV}, 6\,\mathrm{TeV}))$

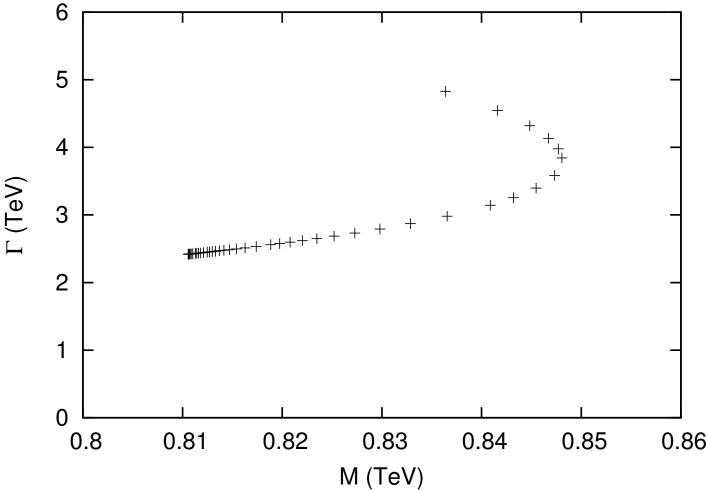

Equivalence Theorem

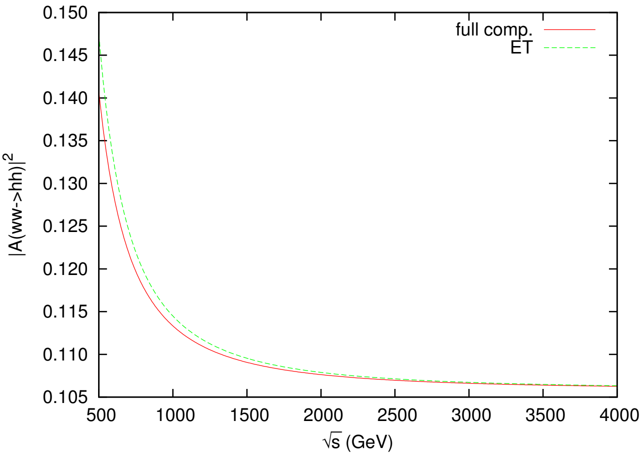

Comparison between the full LO $\omega\omega \to hh$ ($\cos\theta = 3$) and that computed through the ET. The SM is used here. Work in collaboration with S. Moretti, to test a modified version of MadGraph.

Equivalence Theorem

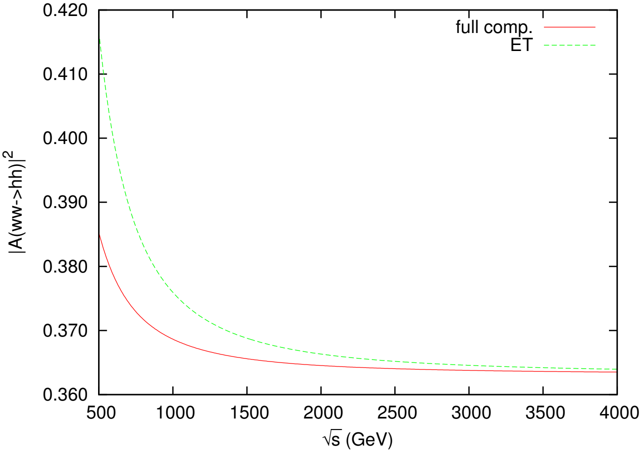

Comparison between the full LO $\omega\omega \to hh$ ($\cos\theta = 6$) and that computed through the ET. The SM is used here. Work in collaboration with S. Moretti, to test a modified version of MadGraph.